

Relaxation oscillators with time delay coupling

Shannon R. Campbell^a, DeLiang Wang^{b,*}

^a Department of Physics, The Ohio State University, Columbus, OH 43210, USA

^b Department of Computer and Information Science and Center for Cognitive Science, The Ohio State University, Columbus, OH 43210, USA

Received 22 August 1996; received in revised form 24 February 1997; accepted 9 June 1997

Communicated by C.K.R.T. Jones

Abstract

We study networks of relaxation oscillators coupled with time delays synapses. A pair of oscillators is analyzed and shown to attain loosely synchronous solutions for a wide range of initial conditions and time delays. Simulations of one- and two-dimensional oscillator networks indicate that locally coupled oscillators are also loosely synchronous. Desynchronous solutions are possible when system parameters are varied. To characterize lossely synchronous networks, we introduce a measure of synchrony, the maximum time difference between any two oscillators. In locally excitatory globally inhibitory oscillator networks with time delays, we find that desynchronous solutions for different groups of oscillators are maintained, and the number of groups that can be segregated is related to the maximum time difference within each group. To examine the maximum time difference, we display its histograms for oscillator networks in one and two dimensions. Also, a range of initial conditions is given so that the maximum time difference is contained as the system evolves.

PACS: 05.45; 87.10; 84.35; 02.30.K

Keywords: Neural networks; Relaxation oscillators; Time delays; Biological oscillations; Synchronization

1. Introduction

Coupled oscillators have been the subject of much research in fields such as physics [17,43], chemistry [1,29], and biology [4,45]. Much recent work into emergent synchronization has been stimulated by observations of synchronous neural activity with frequencies in 30–80 Hz in various brain regions, referred to as 40 Hz oscillations. These studies indicate that neural activity can be synchronized over long distances, e.g., 14 mm in monkey sensorimotor cortex, and across both hemispheres of the brain [32].

Visual features of an object, such as motion, color, and orientation, appear to be processed in distinct cortical areas [46]. The brain is able to group, or link, these features together to create the perception of a coherent object. How the brain links various features to form a coherent object is known as the feature binding problem. Theoreticians have proposed that temporal correlations in the firing patterns of different neurons may serve to link separate features [21,37]. One may implement temporal correlation with neural oscillators. In vision, for example, each element, or pixel of an image, can be represented with an oscillator. A temporal labeling process is then implemented such that all oscillators comprising an object have the same phase. Different objects are represented

* Corresponding author. Tel.: (614) 292-6827; fax: (614) 292-2911; e-mail: dwang@cis.ohio-state.edu.

by different phases of oscillation. This particular form of temporal correlation is referred to as *oscillatory correlation* [36]. Using this concept, oscillator networks performing a variety of perceptual tasks, e.g., sensory segmentation and feature binding, have been proposed [2,11,14,40]. Oscillatory associative memories have also been constructed, and have the benefit that multiple patterns can be recalled simultaneously [35,41].

Time delays in signal transmission are inevitable in both the brain and physical systems. In unmyelinated axons, the speed of signal conduction is approximately 1 mm/ms [13]. Connected neurons which are 1 mm apart may have a time delay of approximately 4% of the period of oscillation (assuming 40 Hz oscillations). How long range synchronization is achieved in the presence of significant time delays is an important question. Furthermore, in any physical implementation (such as analog VLSI) of an oscillator network, transmission delays are unavoidable. Since even small delays may alter the dynamics of differential equations with time delays [16], it is necessary to understand how conduction delays change the behavior of oscillator networks.

The inclusion of time delays in a differential equations can cause a stable point to destabilize, an unstable point to become stable [12,20], and in other cases, chaos can emerge in a system that would otherwise be described by a stable fixed point [31]. To illustrate the effects time delays may have, we discuss the following equation:

$$\dot{x}(t) + 2\dot{x}(t) = -x(t).$$

The above equation has an asymptotically stable fixed point at zero. A trajectory for the above equation is the thick curve displayed in Fig. 1. If one introduces a time delay,

$$\dot{x}(t) + 2\dot{x}(t - \tau) = -x(t)$$

then the trivial solution becomes unstable for any positive delay τ [16]. One such trajectory for this time delay differential equation is the thin curve in Fig. 1.

In this paper we study relaxation oscillators with time delay coupling. Relaxation oscillators have properties of fast synchrony when compared to

nonrelaxation type, such as sinusoidal oscillators [33,34,36,39]. This is an important distinction. If oscillatory correlation is to be used to support perception or in an engineering system, e.g., computer vision, then synchronization must occur quickly to be useful in a rapidly changing environment. In many studies of oscillator networks [3,14,38], simulations were displayed that indicated synchrony, but the rate at which the networks attain synchrony and the size of the networks that can synchronize were not studied. Furthermore, how the rate of synchronization changes with the number of oscillators was not examined. Terman and Wang [36] showed that a network of locally coupled relaxation oscillators achieves synchrony at an exponential rate, independent of the number of oscillators, or the dimension of the network.

To implement oscillatory correlation effectively, a robust and quick method of desynchronization must also exist. Several authors have proposed models that perform both synchronization and desynchronization [2,28,38]. However, the process of separating groups of oscillators was shown in simulations, but not analyzed. Terman and Wang [36] proved that desynchronization is achieved in their locally excitatory globally inhibitory oscillator network (LEGION) [42]. A global inhibitor, connected with all oscillators, is able to desynchronize groups of oscillators without destroying synchrony within a group. It is further shown that n groups can be separated in at most n cycles. LEGION is able to quickly synchronize a group of oscillators, as well as desynchronize different groups of oscillators. These properties are thoroughly understood analytically. Due to these unique properties, we have chosen to examine the effects of time delays in relaxation oscillators.

To our knowledge, time delays in networks of relaxation oscillators have not been extensively studied. In [9], a perturbation analysis was carried out for coupled relaxation oscillators with time delays. The coupling was assumed to be small and the interaction term was not based on excitatory chemical synapses, as is ours. Due to the differences in the coupling term, it is not surprising their results do not agree with ours. Studies of time delays in other oscillator networks have revealed a diverse and interesting range of behaviors. In

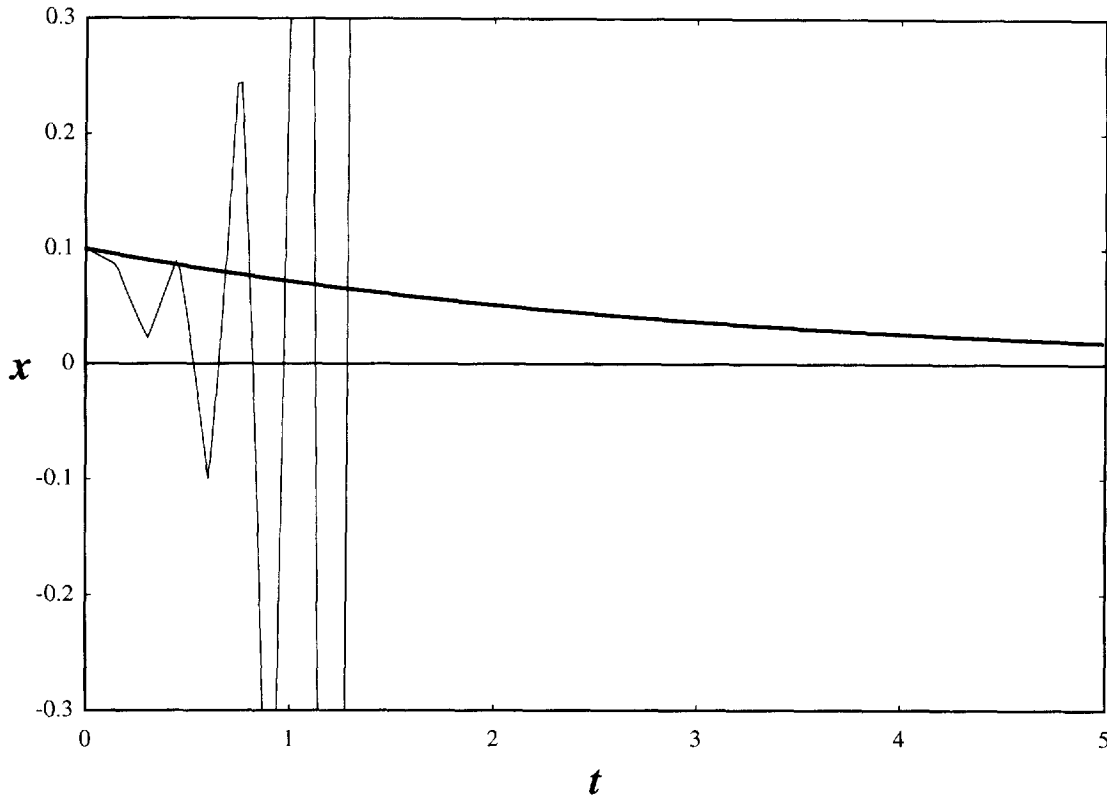


Fig. 1. A trajectory of x is plotted as a function of t without time delay (thick curve) and with time delay (thin curve), using $\tau = 0.15$. The latter trajectory quickly grows beyond the boundaries of the box and begins to appear as a sequence of nearly vertical lines.

a network of identical phase oscillators with local coupling, the inclusion of a time delay in the interactions decreases the frequency [24]. A network of phase oscillators with pulsatile coupling is known to synchronize perfectly with excitatory couplings and no time delay [22]. However, if time delays are included in this same network, clusters of synchronous oscillators form, but become desynchronized after a time [6]. If the coupling is changed to be inhibitory, stable synchronous groups of oscillators emerge. Furthermore, in time delay systems one must specify initial conditions during the time $[-\tau, 0]$. Different initial conditions may lead to different asymptotic behaviors [8]. See [5,19,20,26,30] for examples of delays in differential equations.

In this paper, the dynamics of relaxation oscillators without time delay coupling is first described

in Section 2. In Section 3 we present analysis for a pair of relaxation oscillators with time delay coupling. We show that loose synchrony is possible for a wide range of initial conditions and time delays. In Section 4 we describe that the dynamics of one- and two-dimensional oscillator networks is similar to that of a pair of oscillators. Here we define our measure of synchrony for networks of oscillators. We also show a simulation of LEGION with time delay coupling between oscillators, and suggest that its properties of grouping oscillators together and desynchronizing different oscillator groups are maintained. In Section 5 we study our measure of synchrony for one- and two-dimensional networks of oscillators. A particular case of initial conditions is discussed, where the degree of synchrony does not degrade as the network evolves. Section 6 concludes the paper.

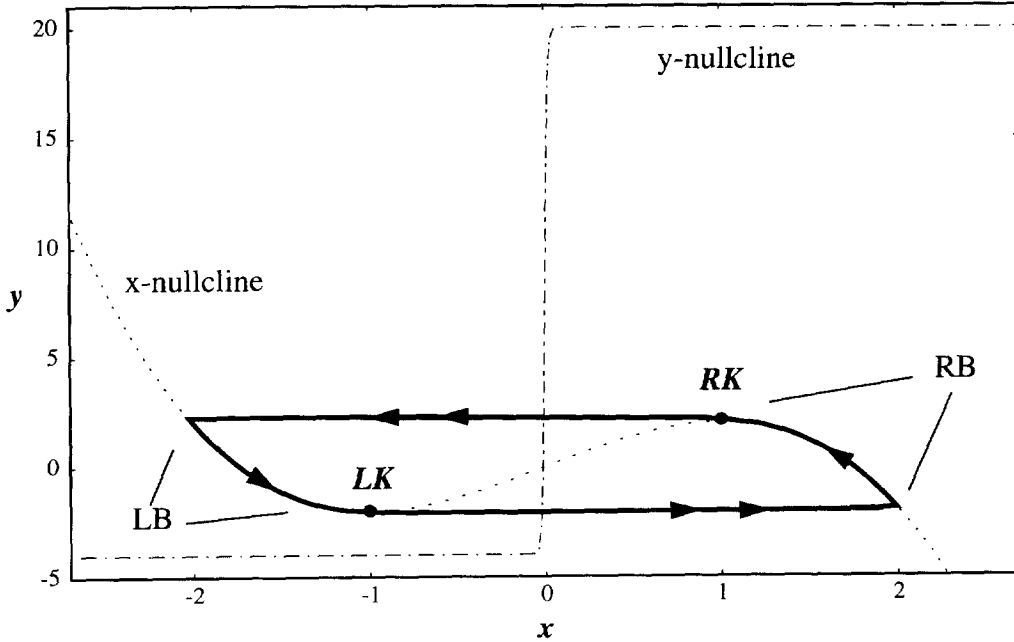


Fig. 2. A plot of the nullclines and limit cycle of a relaxation oscillator defined in (1). The dotted curve is the x -nullcline and the dash-dot curve is the y -nullcline. The thick solid curve represents the limit cycle, which is the result of numerical calculation. The parameters used are $\lambda = 8$, $\gamma = 12$, $\varepsilon = 0.005$, and $\beta = 1000$.

2. Basic dynamics of neural oscillators

Before treating the dynamics of relaxation oscillators coupled with time delays, it is useful to describe their dynamics without time delays. We examine a specific oscillator model. A more general description of a pair of coupled relaxation oscillators can be found in [33]. The oscillator we study is defined as

$$\dot{x} = 3x - x^3 - y, \quad (1a)$$

$$\dot{y} = \varepsilon(\lambda + \gamma \tanh(\beta x) - y). \quad (1b)$$

These functions are equivalent to those used in [36]. The x -nullcline, $\dot{x} = 0$, is a cubic function. Two important values of this cubic are the y -values of the local extrema. In Fig. 2 the extrema are denoted by **RK** (right knee) and **LK** (left knee). The y -nullcline, $\dot{y} = 0$, is a sigmoid and is assumed to be below the left branch (LB) and above the right branch (RB) of the cubic as shown in Fig. 2. The parameter β controls the steepness of the sigmoid and we use $\beta \gg 1$. The value ε is chosen to be small, $0 < \varepsilon \ll 1$, so x is

a fast variable and y is a slow variable. The oscillator thus defined is a typical relaxation oscillator. The limit cycle is made up of four pieces: two slowly changing pieces along the LB and RB, and two fast pieces that connect the left and right solutions. The parameters λ and γ are used to modify the amount of time an oscillator spends in the left and right branches. The trajectory and nullclines for this oscillator are shown in Fig. 2. The parameter values used to produce these specific curves are given in the caption of Fig. 2.

To illustrate the coupling, we examine two oscillators, defined as

$$\dot{x}_1 = 3x_1 - x_1^3 - y_1 + \alpha S(x_2), \quad (2a)$$

$$\dot{y}_1 = \varepsilon(\lambda + \gamma \tanh(\beta x_1) - y_1), \quad (2b)$$

$$\dot{x}_2 = 3x_2 - x_2^3 - y_2 + \alpha S(x_1), \quad (2c)$$

$$\dot{y}_2 = \varepsilon(\lambda + \gamma \tanh(\beta x_2) - y_2). \quad (2d)$$

The value α is the coupling strength, and the interaction term is a sigmoid, $S(x) = [1 + \exp(\kappa(\theta - x))]^{-1}$, mimicking excitatory synaptic coupling. The value of

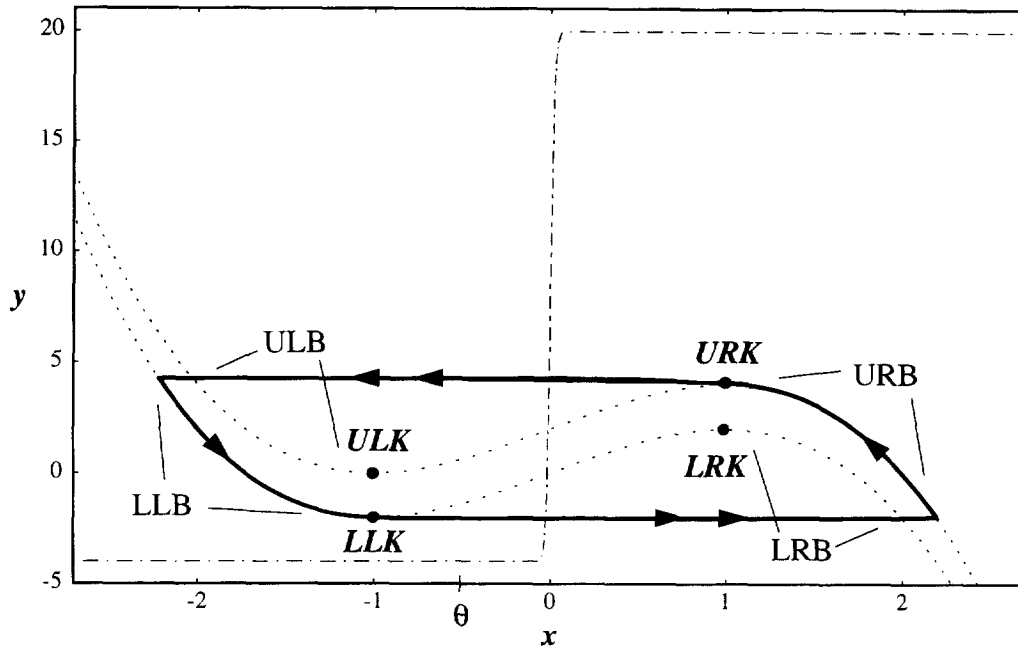


Fig. 3. A plot of the nullclines and limit cycle for a pair of relaxation oscillators as defined in (2). See the caption of Fig. 2 for curve conventions. All trajectories in this figure are the result of numerical calculation. The parameters used are $\alpha = 2$, $\theta = -0.5$, and $\kappa = 500$, with the other parameters as listed in the caption of Fig. 2.

κ modifies the steepness of this sigmoid and we use $\kappa \gg 1$. Increasing the value of $\alpha S(x)$ results in a raise of the x -nullcline, $\dot{x}_i = 0$. This is a property seen in several descriptions of neural behavior [7,10,23,44]. In the limit, $\varepsilon \rightarrow 0$, with the threshold of the interaction term, θ , between the outer branches of the cubic, the system behaves as if $S(x)$ is a step function. Thus the interaction is either nonexistent, or excitatory. When an oscillator travels from a LB to a RB, the other oscillator receives excitation. The excitation raises the x -nullcline of the oscillator. The excited oscillator then exhibits dynamics based on its modified phase space, a mechanism referred to as fast threshold modulation [33]. The three pertinent nullclines for this system are pictured in Fig. 3. As before, the pertinent values of the x -nullclines are the y -values of their local extrema. For the particular equations we use in (2), the x -nullcline shifts upward in direct proportion with a change in $\alpha S(x)$. The local extrema are denoted by the lower left knee (**LLK**) and the lower right knee (**LRK**) for the unexcited x -nullcline, and the upper left

knee (**ULK**) and the upper right knee (**URK**) for the excited nullcline. The values of the extrema for the x -nullclines given in (2) are:

$$\mathbf{LLK} = (LLK_x, LLK_y) = (-1, -2),$$

$$\mathbf{LRK} = (LRK_x, LRK_y) = (1, 2),$$

$$\mathbf{ULK} = (LLK_x, LLK_y + \alpha),$$

$$\mathbf{URK} = (LRK_x, LRK_y + \alpha).$$

The term 'jump' is used when an oscillator moves from either of the LBs to either of the RBs, or vice versa. The term 'hop' is used to describe the relatively smaller movements when an oscillator moves from an upper to a lower branch, or vice versa. Also, when an oscillator is on either of the LBs, we say that it is in the silent phase and when an oscillator is on either of the RBs, we say that it is in the active phase.

A basic description of the behavior of (2) now follows. Let the oscillators be denoted O_1 and O_2 . Let both oscillators begin on the lower left branch (LLB), with $y_2 > y_1$. We assume that the time an oscillator

spends traveling along LLB is longer than the time an oscillator spends on the upper right branch (URB). Because the motion is counter-clockwise along the limit cycle O_1 leads O_2 . The leading oscillator, O_1 , will reach LLK_y first, and jump up to the lower right branch (LRB). There are four basic trajectories that can arise based on the position of O_2 at the time O_1 jumps up. Somers and Kopell [33] have described similar trajectories, so we give only a brief summary here. If O_2 is below $LLK_y + \alpha$, it will jump up to URB. When O_2 crosses the interaction threshold, O_1 will hop from LRB to URB. The order of the oscillators is reversed for this case. If, however, O_2 is above $LLK_y + \alpha$ when O_1 jumps up, O_2 will hop to the upper left branch (ULB). Its motion will continue along ULB until it reaches $LLK_y + \alpha$, at which time it will jump up to URB. There are two possibilities for the relative positions of the oscillators on the active phase: the order may be reversed or not. This accounts for two more cases. The fourth trajectory occurs when O_1 jumps up, and O_2 is above $LLK_y + \alpha$ by such an amount that it is possible for O_1 to traverse the active phase, and return to the silent phase before O_2 can jump up. Parameters can be found so that each case results in a significant phase contraction between the two oscillators. Terman and Wang [36] showed that rapid synchrony is achieved in a network of locally coupled relaxation oscillators. This fast synchrony is independent of the dimension, or the size of the network.

3. Dynamics including time delay

3.1. Singular solutions

We now introduce a time delay in the interactions. The equations are:

$$\dot{x}_1 = 3x_1 - x_1^3 - y_1 + \alpha S(x_2(t - \tau)), \quad (3a)$$

$$\dot{y}_1 = \varepsilon(\lambda + \gamma \tanh(\beta x_1) - y_1), \quad (3b)$$

$$\dot{x}_2 = 3x_2 - x_2^3 - y_2 + \alpha S(x_1(t - \tau)), \quad (3c)$$

$$\dot{y}_2 = \varepsilon(\lambda + \gamma \tanh(\beta x_2) - y_2), \quad (3d)$$

The time delay is only in the interaction between the x variables. The fast system of (3) is obtained by setting $\varepsilon = 0$. This results in

$$\dot{x}_i = 3x_i - x_i^3 - y_i + \alpha S(x_j(t - \tau)), \quad (4a)$$

$$\dot{y}_i = 0, \quad (4b)$$

where $i = 1, 2$ and $j = 3 - i$. The slow system for (3) is derived by introducing a slow time scale $t' = \varepsilon t$ and then setting $\varepsilon = 0$. The slow system for LLB is

$$\dot{x}_i = h(y_i), \quad (5a)$$

$$\dot{y}_i = \lambda + \gamma \tanh[\beta h(y_i)] - y_i, \quad (5b)$$

where $x = h(y)$ describes LLB of (3). System (5) determines the slow evolution of an oscillator on the LLB. Because $\beta \gg 1$ and $h(y) \leq -1$, we rewrite (5b) as

$$\dot{y}_i = \lambda - \gamma - y_i. \quad (6)$$

For an oscillator on ULB, (6) will again result because $h_e(y) \leq -1$, where $x = h_e(y)$ defines the ULB. Thus an oscillator has the same velocity in the y -direction along either of LBs. For RBs, these same steps result in the following analogous equation:

$$\dot{y}_i = \lambda + \gamma - y_i. \quad (7)$$

The velocity in the y -direction of an oscillator along either of RBs is given by (7). Because of this, the hops that occur along the upper and lower cubics do not affect the time difference between the two oscillators. Only the jumps from a LB to a RB and vice versa can result in changes in the time difference between the two oscillators. In more generalized versions of relaxation oscillators, the speed along different cubics may be different. We briefly address this issue in Section 3.4.

In the singular limit, $\varepsilon = 0$, system (3) reduces to two variables. The exact form of the x -nullcline is not important as long as a general cubic shape is maintained. The evolution of the system is determined by solving (6) and (7). The equation describing $y_i(t)$ along either of the LBs is

$$y_i(t) = (y_i(0) - \lambda + \gamma)e^{-t} + \lambda - \gamma. \quad (8)$$

The y -position of an oscillator along either of the RBs is given by

$$y_i(t) = (y_i(0) - \lambda - \gamma)e^{-t} + \lambda + \gamma. \quad (9)$$

We compute T , the total period of oscillation using (8) and (9), for a loosely synchronous solution. The time it takes to travel from LLK_y to $LRK_y + \alpha$, along URB, is given by

$$\tau_{\text{URB}} = \log \left(\frac{LLK_y - \gamma - \lambda}{LRK_y + \alpha - \gamma - \lambda} \right). \quad (10)$$

The time it takes to travel from $LRK_y + \alpha$ to LLK_y , along LLB, is given by

$$\tau_{\text{LLB}} = \log \left(\frac{LRK_y + \alpha + \gamma - \lambda}{LLK_y + \gamma - \lambda} \right). \quad (11)$$

Thus, we have $T = \tau_{\text{URB}} + \tau_{\text{LLB}}$.

Our analysis in this section and Section 3.2 is derived at the singular limit, i.e. $\varepsilon = 0$. We have not carried out a perturbation analysis. We note, however, that Terman and Wang [36] have carried out an analysis of networks of relaxation oscillators in the singular limit and extended their analysis from $\varepsilon = 0$ to small positive ε . Our networks differ from theirs in the inclusion of time delays between the oscillators, but it may be possible that a singular perturbation analysis can be carried out similarly. We have done substantial testing with various values of ε . Our results indicate that values of $0 < \varepsilon \ll 1$ do not significantly alter any of the dynamics discussed.

3.2. Loosely synchronous solutions

As part of our analysis, we need a measure of the distance between the two oscillators. The Euclidean measure of distance does not yield intuitive results because of the constantly changing speed of motion along the limit cycle. We instead use the time difference between the two oscillators, $\Gamma(y_1(t), y_2(t))$ [18,36]. This function measures the time it takes an oscillator at $y_2(t)$ to travel to $y_1(t)$ and is only valid if both oscillators are on the same branch of the limit cycle. In this paper two oscillators are defined to be *loosely synchronous* if the time difference

between them is less than or equal to the time delay, or $\Gamma(y_1(t), y_2(t)) \leq \tau$.

We describe various solutions for (3) in the singular limit, but only for a set of specific initial conditions and a limited range of time delays. We assume that both oscillators lie on LLB so that they are on the limit cycle during the time $[-\tau, 0]$ with $y_2 > y_1$. The maximum initial time difference is $\tau_{\text{LLB}} - \tau$. By restricting the initial conditions in this manner, the behavior of the system is determined by two parameters; the initial time difference between the two oscillators and the time delay. In broad regions of this parameter space we find distinct classes of trajectories. For some of these classes we are able to calculate the time difference between the two oscillators. For other regions we rely on numerical simulations to indicate the final state of the system. In Fig. 4 we summarize five regions of the parameter space that we have examined. In regions I–IV we show that loosely synchronous solutions arise provided that the coupling strength is appropriately bounded. Numerical simulations in region V indicate that antiphase solutions of high frequency can result. We examine time delays in the range $0 - \tau_{\text{RM}}$. The value τ_{RM} (the subscript RM stands for right minimum) is the time needed to traverse the fastest branch in the system, which in our system is LRB, and is given by

$$\tau_{\text{RM}} = \log \left(\frac{LLK_y - \lambda - \gamma}{LRK_y - \lambda - \gamma} \right). \quad (12)$$

This value can be a significant portion of the period of oscillation and we present analytic results within this range. Numerical simulations indicate that for $\tau > \tau_{\text{RM}}$, loose synchrony is not commonly achieved.

We first describe region I of Fig. 4. Here the oscillators have an initial time difference of less than equal to τ , or $\Gamma(y_1(0), y_2(0)) \leq \tau$. In this situation, O_2 will jump up to LRB before receiving excitation. Thus, the only effect of the interaction is to cause O_2 to hop from LRB to URB. Since this hop does not affect the speed of an oscillator in the y -direction, or its y -value, it has no effect on the time difference between the two oscillators. In this region the oscillators have simple periodic motion and maintain a constant time difference. Any small perturbation within this region changes the time difference; thus region I is neutrally

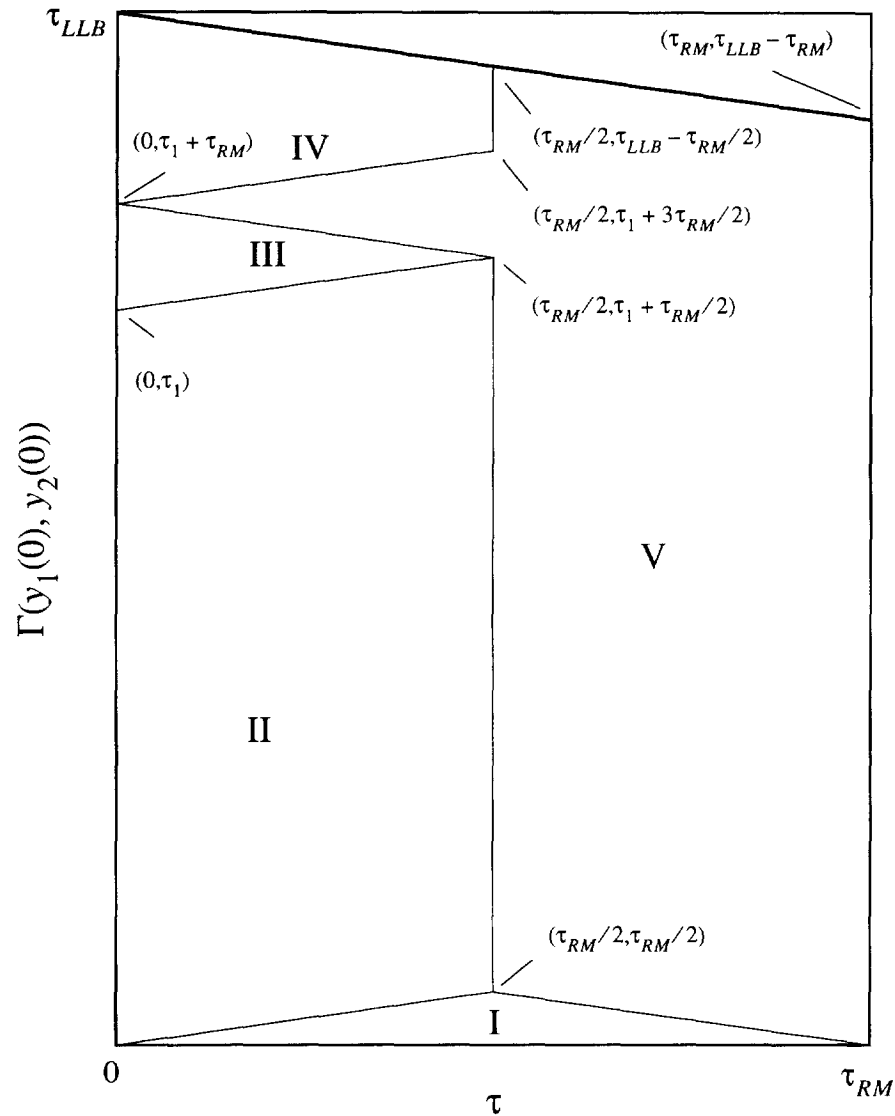


Fig. 4. A diagram in parameter space indicating regions of distinct behaviors. Regions I–IV are distinguished by specific classes of trajectories and these regions result in loosely synchronous solutions. Numerical simulations indicate that much of region V consists of desynchronous solutions. The unlabeled region is not analyzed because it contains initial conditions which do not lie on the limit cycle for a given value of the time delay. The axes do not have the same scale. The equations specifying the boundaries of regions I–IV are given in Section 3 and also in Appendix A.

stable. Solutions in region I are always loosely synchronous. Typical trajectories for a pair of oscillators in region I are shown in Fig. 5(A). There are two boundaries for region I, and the first is given simply by $\Gamma(y_1(0), y_2(0)) \leq \tau$ for $0 \leq \tau < \tau_{RM}/2$. For time delays larger than $\tau_{RM}/2$, there is a different relation between the initial separation and the time delay. In

order for loose synchrony to occur, we must ensure that O_1 does not traverse LRB and jump down to LLB before receiving excitation. This condition results in $\Gamma(y_1(0), y_2(0)) + \tau < \tau_{RM}$ for $\tau_{RM}/2 \leq \tau < \tau_{RM}$. If $\Gamma(y_1(0), y_2(0)) + \tau \geq \tau_{RM}$, then O_1 receives excitation after it has jumped down to LLB. For this case, one oscillator is in the silent phase, and the other

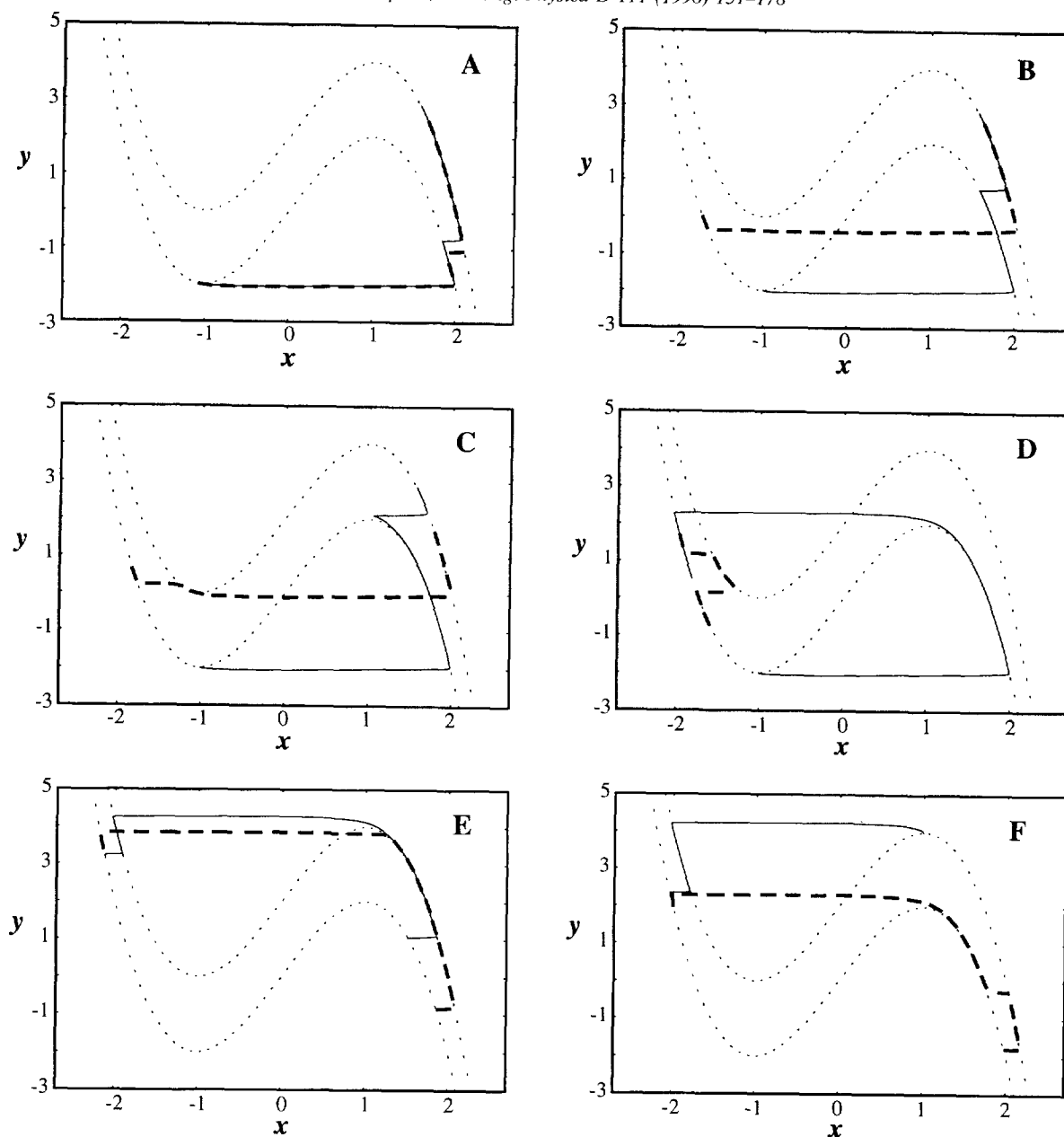


Fig. 5. Plots of trajectories in x and y space for various classes of initial conditions. All trajectories are numerically calculated using parameters listed in the captions of Figs. 2 and 3 with a time delay of $\tau = 0.03T$ and $\alpha = 2$. The thin solid curve represents the trajectory of O_1 , which is always the first oscillator to jump-up in (A), (B), (C), and (D). O_1 is also the first oscillator to jump-down in (E) and (F). The thick dashed curve represents the trajectory for O_2 . (A) This graph displays typical trajectories for a pair of oscillators whose initial time difference is in region I of Fig. 4. (B) Trajectories for a pair of oscillators whose initial time difference is in region II. (C) Trajectories for region III. (D) Trajectories for region IV. In this region it is possible for antiphase solutions to arise if the coupling strength is not large enough. In (E) and (F) we display the two classes of trajectories arising when two oscillators jump-down from the active phase to the silent phase of the limit cycle. (E) This graph displays the trajectories for a typical initial condition as described in Appendix B and is analogous to region II of Fig. 4. (F) This graph displays the trajectories for the oscillators as they jump-down from RBs to LBs with initial conditions analogous to region III of Fig. 4.

oscillator is in the active phase. Numerical simulations indicate that desynchronous solutions typically result from this type of trajectory.

Region II of Fig. 4 contains trajectories such that when O_2 receives excitation, it is able to immediately jump up to URB, and O_1 receives excitation at time 2τ . If $\tau > \tau_{RM}/2$, then O_1 jumps down to LRB and one oscillator is in the silent phase and the other oscillator is in the active phase. As previously noted, desynchronous solutions typically result from this type of trajectory. However, if the time delay satisfies $0 \leq \tau < \tau_{RM}/2$, then O_1 hops from LRB to URB when it receives excitation and both oscillators are on URB. The evolution of the system can then readily be calculated. Region II is thus defined for time delays $0 \leq \tau < \tau_{RM}/2$. Typical trajectories for a pair of oscillators in this region are shown in Fig. 5(B). The initial time difference is bounded by $\tau < \Gamma(y_1(0), y_2(0)) \leq \tau_1 + \tau$, where τ_1 is given by

$$\tau_1 = \log \left(\frac{LLK_y + \alpha - \lambda + \gamma}{LLK_y - \lambda + \gamma} \right). \quad (13)$$

This is the time of travel from $LLK_y + \alpha$ to LLK_y on LLB. With zero time delay, the y -distance between the two oscillators remains the same before and after the jump up, but the time difference between them changes. If the ratio of the initial time difference on LLB to the time difference after the jump (on URB) is less than 1, then there is compression [33], and the oscillators synchronize at a geometric rate. With time delay, the y -distance between the two oscillators changes before they are both on URB. From Fig. 5(B), one can see that O_1 travels upward on LRB, while O_2 travels downward on LLB until receiving excitation. Depending on the initial conditions, the y -distance between the two oscillators can shrink, or increase. When the y -distance decreases, the time difference decreases by a factor greater than the compression ratio alone. When the y -distance increases, the time difference is less than or equal to the time delay. In Appendix A, we derive the time difference between the two oscillators after one period, and show that it decreases.

The initial conditions of region III of Fig. 4 are bounded by $\tau_1 + \tau < \Gamma(y_1(0), y_2(0)) < \tau_1 + \tau_{RM} - \tau$.

In region III, O_2 receives excitation, hops to ULB, and jumps up to URB before O_1 jumps down to LLB. Typical trajectories for a pair of oscillators in region III are shown in Fig. 5(C). For this class of trajectories, it is shown in Appendix A that after one cycle, the time difference between the two oscillators decreases.

Region IV of Fig. 4 is bounded by $\tau_1 + \tau_{RM} + \tau < \Gamma(y_1(0), y_2(0)) \leq \tau_{LLB} - \tau$. If the initial separation of the oscillators is larger than the upper bound, then the oscillators cannot be on the limit cycle and on the LLB during the time $[-\tau, 0]$, and we do not examine initial time differences beyond this range. In region IV, O_2 receives excitation and hops to ULB. However, O_2 does not receive excitation long enough to reach $LLK_y + \alpha$ and hops back to LLB after O_1 has traversed LRB. Typical trajectories for a pair of oscillators in region IV are shown in Fig. 5(D). In Appendix A we show that the time difference between the two oscillators decreases if the coupling strength is sufficiently large, i.e. satisfies condition (A.35). We also show that if that condition is met, then the oscillators whose initial conditions are in region IV do not map into region V, but instead map to regions I, II, or III. If condition (A.35) is not satisfied then desynchronous solutions can occur for some initial conditions.

The analysis of regions II–IV of Fig. 4 requires that we calculate the change in the time difference between the two oscillators when they jump down from the active to the silent phase as well. We do this in Appendix B. The cases examined are analogous to regions II and III and are called region II_R and III_R. In Fig. 5(E) we display trajectories for a pair of oscillators in region II_R. The leading oscillator in this region jumps down and the other oscillator is able to jump down from URB to LLB when it no longer receives excitation. In region III_R the leading oscillator jumps down and the other oscillator hops from URB to LRB when it no longer receives excitation and then jumps to LLB. Typical trajectories for a pair of oscillators in region III_R are shown in Fig. 5(F). We assume that LRB is the fastest branch in the system. This places a limit on the size of α , and also limits the number of trajectories that can arise from the RBs. The resulting restriction on α is given in (B.14). Both restrictions,

(A.35) and (B.14), on the coupling strength are summarized to

$$\sqrt{\frac{c_2 c_3 c_4}{c_1}} e^{-\tau} - c_2 < \alpha < \frac{c_1 c_2 - c_3 c_4}{c_3 - c_1}, \quad (14)$$

where the values of c_i are given by

$$\begin{aligned} c_1 &= LLK_y - \lambda - \gamma, & c_5 &= LLK_y + \alpha - \lambda - \gamma, \\ c_2 &= LLK_y - \lambda + \gamma, & c_6 &= LLK_y + \alpha - \lambda + \gamma, \\ c_3 &= LRK_y - \lambda - \gamma, & c_7 &= LRK_y + \alpha - \lambda - \gamma, \\ c_4 &= LRK_y - \lambda + \gamma, & c_8 &= LRK_y + \alpha - \lambda + \gamma. \end{aligned}$$

For the parameters listed in the caption of Fig. 7, for example, the coupling strength must be within the following values $1.1334 < \alpha < 16$ according to (14). Note that in the case of zero time delay, the conditions in (14) must still be satisfied in order for loose synchrony (in this case perfect synchrony) to occur.

Within the bounds specified in (14), and given initial conditions in regions II–IV of Fig. 4, the time difference between the two oscillators will always decrease. As the system evolves, the time difference will decrease until it becomes less than the time delay. The oscillators will then be loosely synchronous.

Note that the diagram obtained in Fig. 4 is not completely generic for all parameter values. One can modify parameters, α , γ , λ , LRK_y , and LLK_y , so that the value of τ_{LLB} changes. This is the value that controls the height of the thick line in Fig. 4. By shifting this line up or down one can change the relative sizes of the regions or even remove region IV. But, since we have assumed that $\tau_{LLB} > \tau_{URB}$ the value of τ_{LLB} cannot be altered so that regions II or III are removed, i.e. $\tau_{LLB} > \tau_1 + \tau_{RM}$. Thus regions II and III always exist. If τ_{LLB} is made larger, then region IV becomes larger, but no new regions are created in this manner.

3.3. Desynchronous solutions

If α is larger than the upper bound in (14), numerical simulations indicate that loose synchrony is still possible. If α is less than the lower bound in (14), then our analysis shows that neutrally stable

desynchronous solutions of period less than T arise for some initial conditions in region of IV of Fig. 4. The period is less than the period of the loosely synchronous solution in part because the oscillators traverse LRB, instead of the longer URB. This desynchronous solution is analogous to a case of antiphase behavior as discussed by Kopell and Somers [15]. In [15] it was stated that antiphase solutions can arise given a coupling strength between relaxation oscillators that is not too large, with limit cycles such that the time spent on the active and silent phases are sufficiently unequal. Our results for region IV are in agreement with these statements. Region IV exists only when the time spent on the silent phase is sufficiently larger than the time spent on the active phase, i.e. $\tau_{LLB} > \tau_1 + \tau_{RM} > \tau_{URB}$, and desynchronous solutions can arise in this region only if the coupling strength is below the lower bound of (14). Because the speed of an oscillator is identical on both upper and lower cubics, these desynchronous solutions are neutrally stable, that is, any small perturbation moves the oscillators into another nearby desynchronous solution. This possibility is also noted in [15]. The range of possible desynchronous solutions does not cover the entire area of region IV. We do not delve further into these particular desynchronous solutions.

In regions I, II, and III of Fig. 4, O_1 always receives excitation before jumping down, and both oscillators are on URB for some amount of time. This situation does not occur in region V and this is the reason why loosely synchronous solutions exhibited in regions I, II, and III, generally disappear in region V. In this region, with time delays larger than $\tau_{RM}/2$, O_1 traverses LRB and jumps down to LLB before receiving excitation. Meanwhile, O_2 receives excitation and jumps to URB. One oscillator is in the silent phase, and the other oscillator is in the active phase, or the oscillators are on the opposite sides of the limit cycle. From these initial conditions, numerical simulations indicate that desynchronous solutions typically arise. They can quickly become perfectly antiphase, with one oscillator receiving excitation and traveling upward along URB, while the other oscillator is not receiving excitation and is traveling downward along

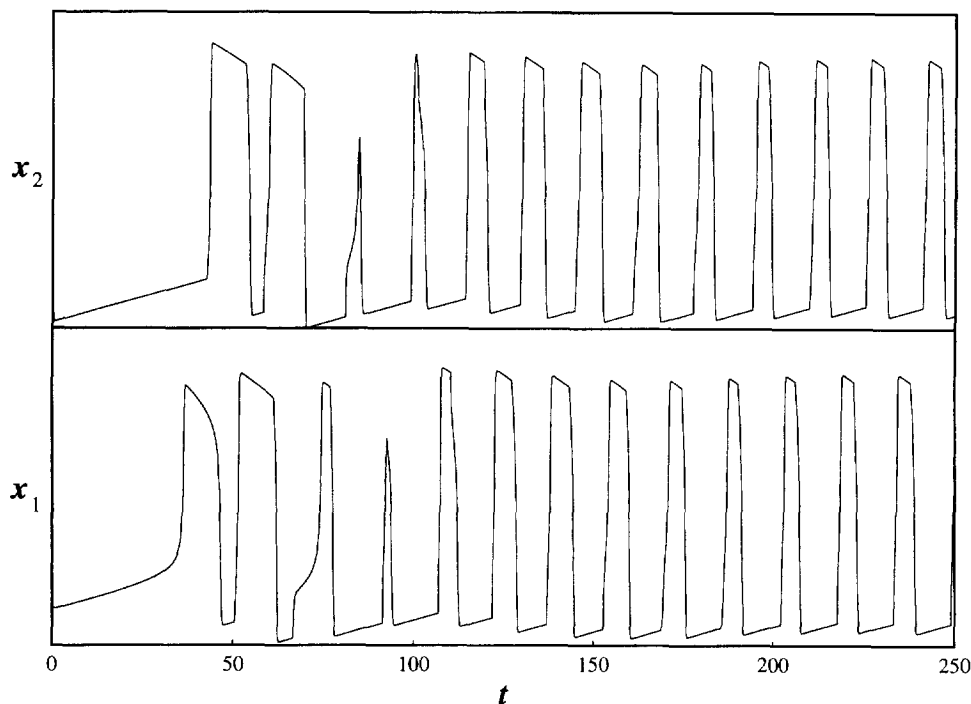


Fig. 6. A plot of antiphase behavior arising in region V of Fig. 4. The parameter values used are listed in the captions of Figs. 2 and 3 with $\tau = 0.07T$, $\alpha = 6$, and $\varepsilon = 0.025$.

LLB. After a time equal to the time delay, the oscillator on the active phase ceases to receive excitation and jumps down to LLB, while the oscillator on the silent phase begins to receive excitation, and jumps up to URB. This solution has period 2τ . The behavior just described is one of many desynchronous solutions that can exist in region V dependent on the location of the knees and the coupling strength. We have obtained some analytic results for a few small convex areas within region V. Our results are not shown here because they do not cover a significant portion of region V. Also, the derivations are quite lengthy. The areas we have examined analytically in region V have desynchronous or antiphase solutions of period less than T . Numerical simulations suggest that region V consists mostly of solutions in which the oscillators are nearly antiphase and have a period less than T . In Fig. 6 we display an example of antiphase behavior in region V. The period of oscillation measured in this figure is approximately 2τ .

3.4. Time delays in other oscillators

For the oscillator model we use, the speed of an oscillator depends only on its y -value, or in other words, the speed of an oscillator is the same no matter which cubic it is on. This condition allows for exact solutions, but is not very general. As noted in [15], different speeds of motion along different cubics can give rise to different behaviors. We have tested this scenario by using the Morris–Lecar equations [23] and other relaxation oscillators that exhibit different speeds along different cubics, and our results from numerical simulations indicate that the predominant behavior of loose synchrony is still observed. A pair of oscillators quickly converges to a solution in which the time difference between the two oscillators is less than or equal to the time delay. However, the loosely synchronous solutions are no longer neutrally stable. We observe several possible solutions for two oscillators, the full analysis of which will be treated elsewhere.

For this paper, it suffices to point out that loose synchrony persists under analogous conditions to those given in Section 3.2.

We find that for initial conditions analogous to region IV of Fig. 4, several desynchronous solutions can exist for small coupling strengths. These solutions are analogous to those described by Somers and Kopell [15], in their analysis of a pair of relaxation oscillators without time delay coupling.

For time delays larger than half the amount of time spent on the fastest branch of the system, we find equivalent behaviors to those observed in region V of Fig. 4. The oscillators frequently exhibit nearly antiphase relations with periods of approximately 2τ , thus conforming to earlier results when the speed of motion is the same for the upper and lower cubics.

In summary, we have analyzed a pair of relaxation oscillators in the singular limit, with initial conditions such that the oscillators are on the silent phase of the limit cycle during the time $[-\tau, 0]$, and with time delays of less than τ_{RM} . Given the appropriate upper and lower bounds on the coupling strength, as specified in (14), loosely synchronous solutions arise for regions I–IV of Fig. 4. For coupling strengths less than the lower bound in (14) and initial conditions such that the time difference between the two oscillators is in region IV, desynchronous solutions can occur. Extensive numerical simulations in region V indicate that loosely synchronous solutions occur, as do antiphase and desynchronous solutions with periods less than T . In numerical studies with Morris–Lecar oscillators and other relaxation oscillators, in which the speed along different cubics is not identical, we find similar results.

4. Networks of oscillators

4.1. Relationship with pairs of oscillators

Analysis of more than two locally coupled oscillators quickly becomes infeasible because the number of possible initial configurations and their resultant possible trajectories increase dramatically with the number of oscillators. The rest of the paper is based on numerical simulations of oscillator networks. The

connection strengths are normalized so that the sum of the weights is the same for every oscillator [40]. For example, in a chain of oscillators, an oscillator at one end receives input from only one oscillator. This connection weight is twice the amount of the connection weight to an oscillator in the center of the chain, which receives input from its two nearest neighbors. Initially, oscillators are randomly placed on LLB of the limit cycle so that the time difference between every pair of oscillators is in regions I–III of Fig. 4. These simulations reveal that the behavior of a network has similarities to that of two oscillators. The most pertinent similarity is that after the network has settled into a stable periodic solution, any two neighboring oscillators i and j have a time difference as follows:

$$|\Gamma(y_i(t), y_j(t))| \leq \tau. \quad (15)$$

In Fig. 7 we demonstrate this behavior by displaying the x -values of a chain of 50 oscillators with nearest neighbor coupling and $\tau = 0.03T$. We use the term loosely synchronous to describe networks of oscillators in which condition (15) is met because each oscillator is still loosely synchronized with its neighbors. In Fig. 7 it appears that the network has stabilized by the 3rd or 4th cycle. In our numerical simulation, we call network stable if the changes in time difference between neighboring oscillators remains below a threshold for more than two periods. This threshold is set to $0.0075T$. With this measure, the network in Fig. 7 meets our criteria of stability by the 3rd cycle.

We have also examined networks in which the connection weights are not normalized, thus the two oscillators at the ends of the chain receive only half as much input as the other oscillators. We find that loose synchrony is achieved so long as the coupling strength to the end oscillators are still within the bounds specified in (14). Also, in tests where 10% noise is added to the coupling strengths and with no normalization, we find that loose synchrony can still be achieved. The oscillators quickly attain solutions such that they are within region I or II with respect to their neighbors, and are thus able to jump when they receive excitation. If the conditions in (14) are not satisfied, then desynchronous solutions can arise. We also note that

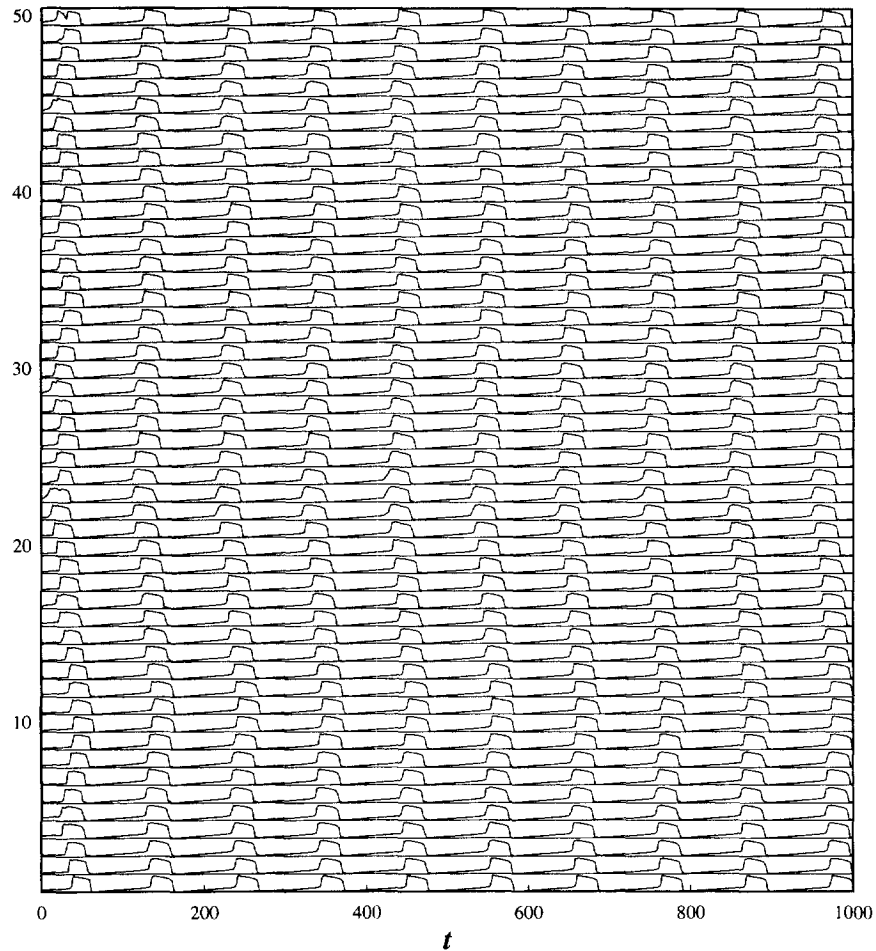


Fig. 7. Loose synchrony in a chain of relaxation oscillators. The temporal activities of 50 oscillators with nearest neighbor coupling are shown. Numerical calculations indicate that this network achieves stability by the 3rd cycle and that all neighboring oscillators satisfy $|F(y_i(t), y_{i+1}(t))| \leq \tau$. The parameter values used are $\lambda = 8$, $\gamma = 12$, $\beta = 1000$, $\kappa = 500$, $\tau = 0.03T$, $\alpha = 6$, $\theta = -0.5$, and $\varepsilon = 0.025$.

similar behaviors hold in networks of relaxation oscillators in which the speed of motion is different for different cubics. Loose synchrony is quickly achieved, but, as in the case for two oscillators, loose synchrony is no longer neutrally stable.

We find through extensive simulations that two-dimensional locally coupled networks also display loose synchrony. In these simulations, all oscillators are randomly distributed on the LLB so that the time difference between every pair of oscillators is within regions I–III of Fig. 4. After the network has achieved

stability, using the same criteria of stability mentioned previously, the time differences between any oscillator and its nearest neighbors are always less than or equal to the time delay. Thus two-dimensional networks also exhibit loose synchrony, similar to a pair of oscillators or a chain. In Fig. 8 we display an example of loose synchrony in a 10×10 network of oscillators. We have combined the x -values of all 100 oscillators in the figure to facilitate the comparison between phases. The network in Fig. 8 meets our criteria of stability by the third cycle.

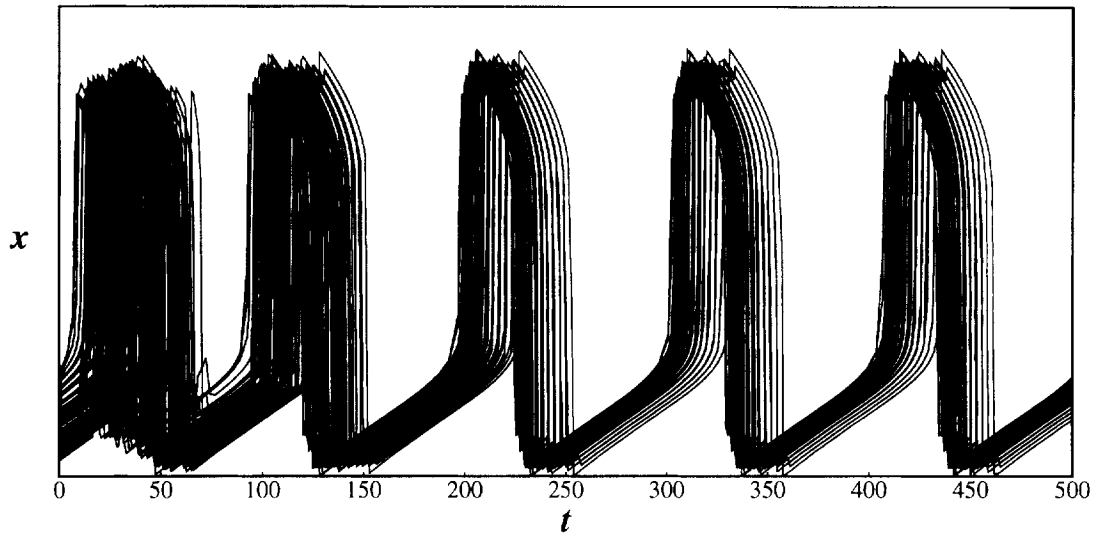


Fig. 8. Loose synchrony in a two-dimensional grid of oscillators. This figure displays the temporal activities of every oscillator from a 10×10 network. Each oscillator is coupled with its four nearest neighbors. The network achieves stability by the third cycle, and for all neighboring oscillators i and j , $|\Gamma(y_i(t), y_j(t))| \leq \tau$. The parameter values used are the same as in Fig. 7.

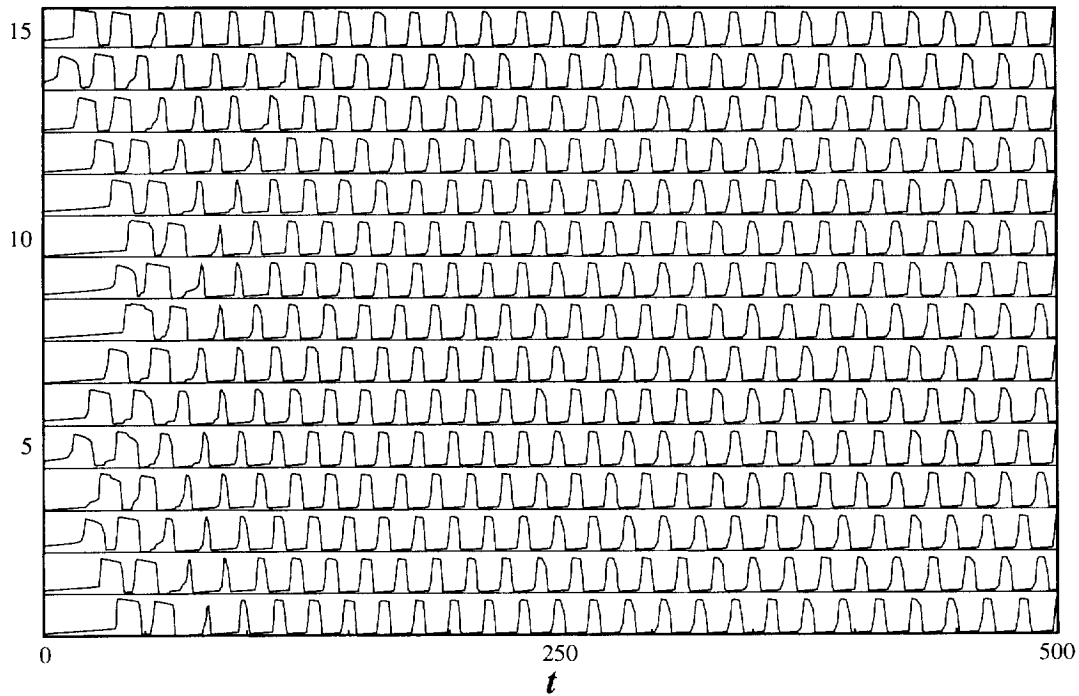


Fig. 9. Antiphase behavior in a chain of relaxation oscillators. The temporal activities of 15 oscillators in a one-dimensional chain with nearest neighbor connections are shown. Neighboring oscillators exhibit antiphase relationships and approach a period of approximately 2τ . The parameter values are listed in the caption of Fig. 7 with $\tau = 0.08T$.

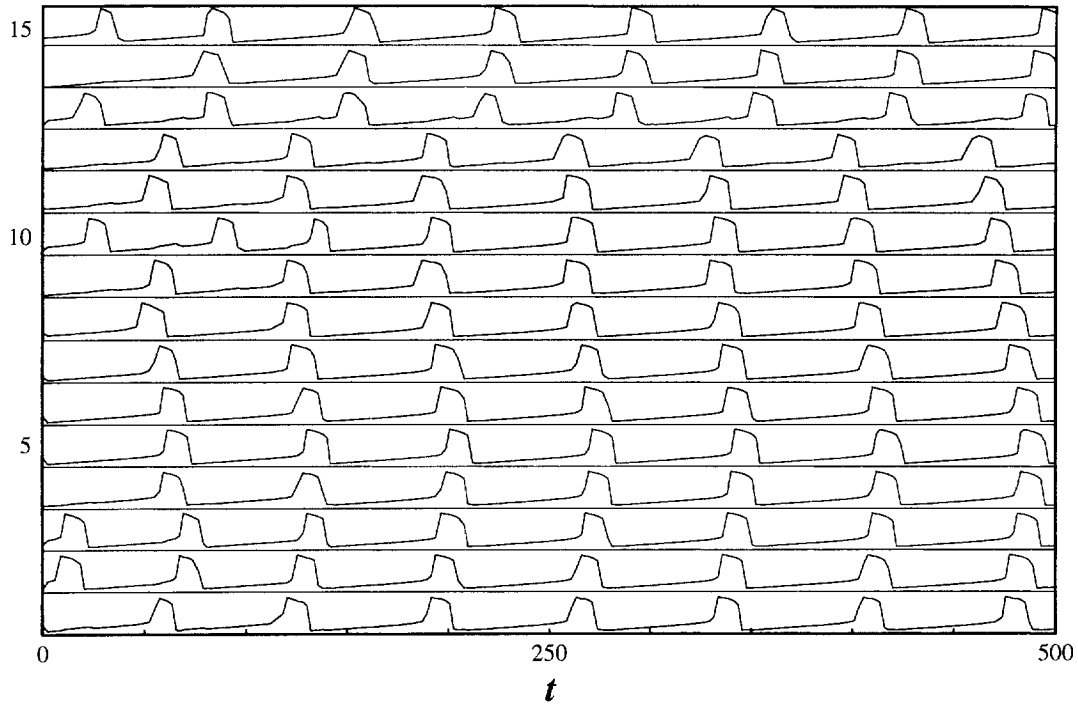


Fig. 10. Desynchronous solutions in a chain of relaxation oscillators. If the coupling strength is below the lower bound specified in (14), desynchronous solutions can arise. In this simulation, $\alpha = 1$, which is below the lower bound specified in (14), and all other parameters are listed in the caption of Fig. 7. Oscillators 12 and 13 had initial conditions such that they are able to remain in a desynchronous relationship. All other neighboring oscillators are loosely synchronous.

In region V of Fig. 4, a pair of oscillators typically exhibits antiphase behavior of high frequency. This behavior can also be seen in networks of oscillators. In Fig. 9 we display an example of antiphase behavior in a chain of 15 oscillators. The oscillators are randomly placed on the LLB of the limit cycle so that the time difference between every pair of oscillators is in region V with $\tau > \tau_{RM}/2$. In this simulation oscillators quickly achieve nearly antiphase relations with their neighbors and the period of each oscillator approaches 2τ .

For small values of the coupling strength, with initial in region IV of Fig. 4, a pair of oscillators can exhibit desynchronous solutions. These conditions can also cause desynchronous solutions in one-dimensional networks. In Fig. 10 we display an example of desynchronous behavior of arising from region IV in a chain of 15 oscillators. The initial

conditions are chosen so that the time difference between every pair of oscillators is randomly distributed in regions I–IV. In Fig. 10 several oscillators initially begin with desynchronous relationships, but become loosely synchronous through interactions with their neighbors. Oscillators 12 and 13, however, remain in a desynchronous relationship, and exhibit the same period of oscillation as the loosely synchronous solutions. This behavior corresponds to fractured synchrony as described in [34]. The correspondence, however, is not exact. Time delays were not studied in [34]. A one-dimensional ring of relaxation oscillators in their system exhibited two distinct groups of oscillators. Each group achieved perfect synchrony and was approximately antiphase with the other group. In our simulation, two groups of oscillators exist in a one-dimensional chain of oscillators. Each group exhibits loose synchrony, and an approximately

antiphase relationship exists between the two oscillators on the single border between the two groups.

For time delays and initial conditions in region V of Fig. 4, there is no clear relation between pairs of oscillators and networks of oscillators. In pairs of oscillators region V consists mostly of antiphase relations. For networks of oscillators loosely synchronous, antiphase, and other solutions arise dependent on the initial conditions and the coupling strength. For the rest of the paper we will focus in the initial conditions and time delays which lead to loose synchrony between neighboring oscillators.

4.2. The maximum time difference

Although simulations indicate that neighboring oscillators are loosely synchronous, loose synchrony does not indicate the degree of global synchrony in an entire network. Obviously, a measure of global synchrony is important, and there are many ways of determining synchrony in an oscillatory system, see [25] for examples. We could convert positions of oscillators on the limit cycle into phase variables, ϕ_j , but due to the large amplitude variations during the hops and jumps, defining a phase is problematic. One could also base a measure on Euclidean distance, and find the average separation between oscillators. However, during the jumps, much distance is covered in a short time. A measure based on Euclidean distance can vary during a single cycle. We instead examine the maximum time difference between any two oscillators in the network. The maximum time difference is defined as follows. Let t_i^k denote the time at which the i th oscillator, O_i , jumps up during the k th period. Let $\Upsilon_{ij}^k = |t_i^k - t_j^k|$ and

$$\Upsilon^k = \max(\Upsilon_{ij}^k) \quad (i, j = 1, \dots, N). \quad (16)$$

Thus, Υ^k is the maximum time difference between any two oscillators during the k th period. Each period of an oscillator can be delineated by the time it jumps up. The initial conditions we use, with the time difference between every pair of oscillators in regions I–III of Fig. 4, allow for this simple definition of the period (see Fig. 7). This measure offers direct comparison

with other pertinent quantities such as the period of oscillation, and the amount of time spent on the active and silent phases. Also, the maximum time difference becomes a constant when the oscillator network achieves stability.

4.3. LEGION with time delay coupling

We first describe LEGION and then, based on numerical simulations, describe how the dynamics of LEGION changes when time delays are included in the interaction between oscillators. The architecture of LEGION is a two-dimensional array of locally coupled relaxation oscillators. In addition, each of the oscillators is coupled with a unit called a Global Inhibitor (GI). Desynchronization is accomplished by GI. Oscillators receiving stimulus become oscillatory and those that do not remain inactive. The connections weights between oscillators are dynamic. The connections between stimulated neighboring oscillators increase to a constant, while connections with unstimulated oscillators decrease to zero. Thus, only stimulated neighboring oscillators are connected. Let us assume that all the oscillators are on the silent phase of the limit cycle. When one oscillator jumps up to the active phase, GI becomes active on the fast time scale and sends inhibition to all oscillators. This inhibition serves to lower the x-nullcline of every oscillator. The x-nullclines of unexcited oscillators are lowered so that they intersect their y-nullclines and the oscillators are attracted to the newly created fixed points. The inhibition from GI, however, is not enough to prevent oscillators receiving excitation from jumping up to the active phase. Thus the oscillator that has jumped up to the active phase, can recruit its stimulated neighboring oscillators. These oscillators jump up to the active phase and recruit their stimulated neighbors and so on. Since each jump decreases the distance between coupled oscillators, a group of stimulated neighboring oscillators quickly synchronizes. Following [36], we refer to a group of stimulated and connected oscillators as a block. A block will jump up to the active phase, while other blocks continue to travel along the silent phase, approaching the attracting fixed points. This mechanism is called selective gating [36]. When a block

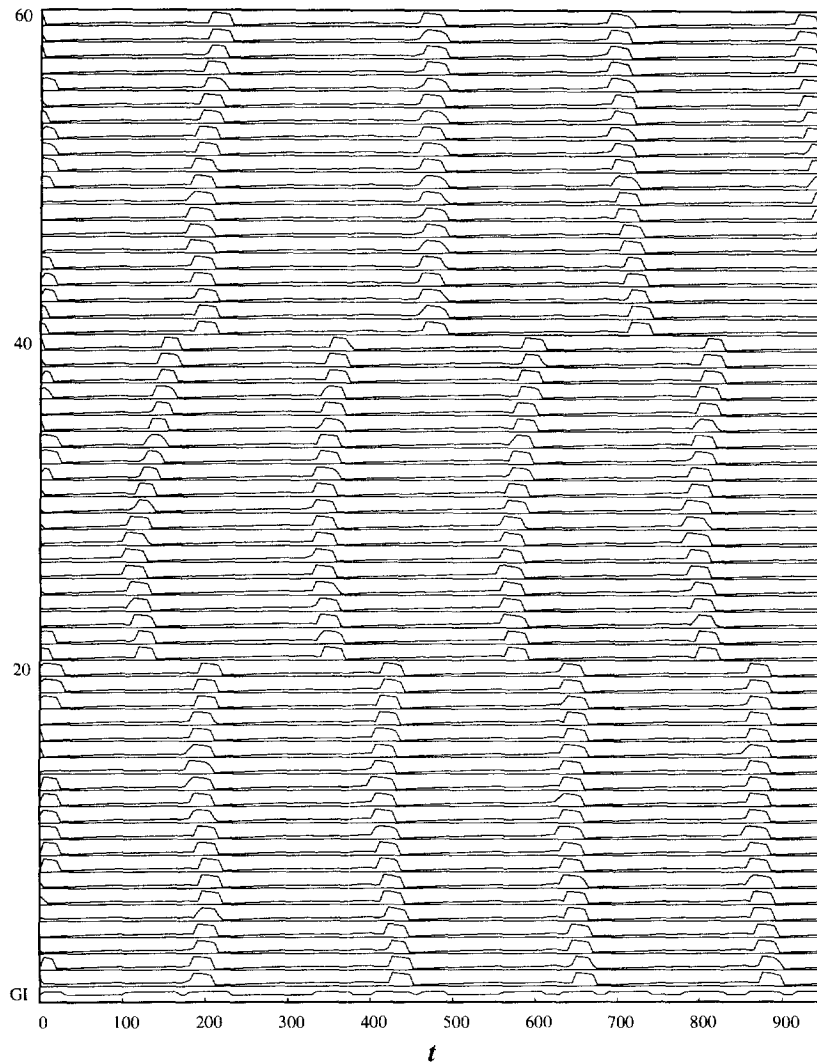


Fig. 11. An example of LEGION dynamics with time delays in the coupling between oscillators. The temporal activity is displayed for 60 oscillators and GI. The activity of GI is displayed beneath the oscillators. The following parameter values are used: $\gamma = 6$, $\lambda = 3.95$, $\alpha = 2$, $\tau = 1$, $\kappa = 500$, $\beta = 1000$, $\theta = -0.5$, and $\varepsilon = 0.025$.

of oscillators jumps down, GI quickly releases its inhibition to the network on a fast time scale. The x-nullclines of all oscillators will then rise so that the attracting fixed points disappear. Other blocks can then jump up to the active phase and the aforementioned process repeats.

Assuming a block of oscillators is perfectly synchronous, the number of blocks that can be desynchronized is related to the ratio of the time an oscillator

block spends on the active and silent phases [36]. If however, a block of oscillators is not perfectly synchronous, the amount of time a block spends in the active phase increases. The amount of time a block spends in the active phase is thus an important measure for the network.

In Fig. 11 we present the output of a network equivalent to LEGION, with the inclusion of time delays between oscillators. Even though all oscillators receive

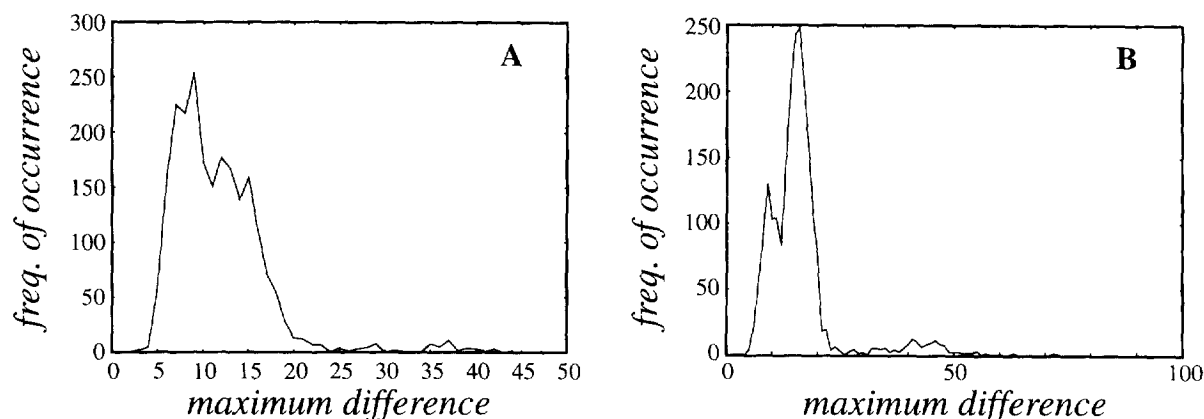


Fig. 12. The histograms of γ^k for one-dimensional networks. The histograms γ^k are based on simulations whose initial conditions were restricted to LLB of the limit cycle so that the time difference between any two oscillators were in regions I–III of Fig. 4. The horizontal axis represents the maximum difference attained, and the vertical axis represent the number of times it was attained. The data were taken after the system had evolved for 11 cycles. The average time needed to achieve stability was approximately three cycles. (A) and (B) are the results for 50 and 100 oscillators, respectively. The data for γ^k in (A) and (B) are based on 2250 and 2160 simulations, respectively. The parameters used are given in the caption of Fig. 7.

stimulation, we set both the connection weights between oscillators 20 and 21, and between those of oscillators 40 and 41, to zero in order to create three groups of oscillators. The network is able to group and segregate the three blocks, but the individual blocks no longer attain perfect synchrony; loose synchrony is achieved within each block. Neighboring oscillators are loosely synchronous according to (15). Because perfect synchrony is no longer achieved, the amount of time that a block of oscillators spends on the active phase is no longer simply determined by that of a single oscillator. The additional amount of time a block spends on the active phase, in comparison with the time a perfectly synchronous block spends on the active phase, is given by the maximum time difference within a block of oscillators. If the maximum time difference for a block is near τ_{LLB} , then the other blocks on the silent phase of the limit cycle become stuck at the attracting fixed points and further segregating them becomes problematic. If, however, the maximum time difference is still relatively small in comparison with τ_{LLB} , then other blocks of oscillators can be separated, and the number of distinct blocks LEGION can segregate does not decrease drastically.

5. Maximum time difference in oscillator networks

5.1. One- and two-dimensional networks

We examine the maximum time difference for one-dimensional networks of oscillators. Since the times at which the oscillators jump up are intrinsically determined by the initial conditions of the network, we cannot determine analytically the value that γ^k will take. Of course, in a chain of N oscillators, the maximum possible value of γ^k is given by $(N - 1)\tau$, but in simulations, we rarely see values of even half of this. We are thus led to examine the distribution of γ^k over a number of trials.

In Figs. 12(A) and (B) we display histograms of γ^k for networks of size 50 and 100 oscillators. The oscillators are placed on LLB so that the initial time difference between every pair of oscillators is randomly distributed in regions I–III of Fig. 4. The largest value γ^1 can have is 21 in the units of Figs. 12(A) and (B). After the network has achieved stability, most of the trials have values of γ^k ($k > 1$) that are less than 21. A small percentage (4%) of the trials resulted in γ^k increasing significantly larger than γ^1 , in some cases almost doubling. Other histograms generated

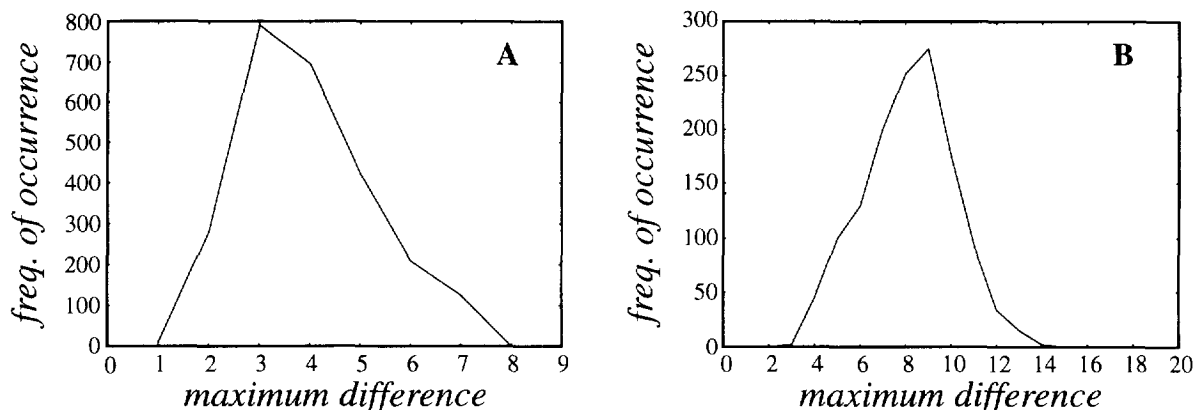


Fig. 13. The histograms of γ^k for two-dimensional networks. These histograms are based on simulations with initial conditions as described in the caption of Fig. 12. The data were taken during the 11th cycle. The average time needed to achieve stability was approximately three cycles. (A) and (B) are the results for 5×5 and 10×10 oscillator networks, respectively. The data for γ^k in (A) and (B) are based on 2530 and 1320 simulations, respectively. The parameter values used are the same as in the caption of Fig. 7.

with different parameter values display similar distributions. By similar we mean that there is a marked tendency for a majority of the trials to remain within the maximum time difference of the initial bounds, or $\gamma^k < \gamma^1$. In addition, there is a small but noticeable peak on the tail of the distribution in Figs. 12(A) and (B). This suggests that there are a few initial conditions which result in large values of the maximum time difference, but we do not know what initial configurations cause this.

We also find in other simulations that the distribution γ^k is sensitive to initial conditions. For initial conditions such that 10% of the oscillators are randomly distributed on URB, the distribution γ^k becomes much broader and the average maximum time difference almost doubles (data not shown).

We now discuss our simulations of two-dimensional networks, in which oscillators are coupled with their four nearest neighbors. The initial conditions are as before, with every oscillator randomly positioned on LLB so that the initial time difference between every pair of oscillators is in regions I–III of Fig. 4. Our simulations indicate that after the network achieves stability, neighboring oscillators have time differences that are less than or equal to the time delay. In other words, the network achieves loose synchrony. As before, the behavior of the maximum time difference is unknown. In Figs. 13(A) and (B) we display histograms of γ^k

for networks of size 5×5 and 10×10 , respectively. Because the coupling is between the four nearest neighbors, the maximum possible difference is given by $(2L - 1)\tau$, where L is the length of one side of a square. As in the histograms for chains of oscillators, the histograms are skewed towards smaller values of the maximum time difference.

We note that, although the network sizes are not large, the above simulations are computationally expensive. Each of the histograms shown in Figs. 12 and 13 require a large number of data points. To collect the data we made use of several hundred high-performance workstations, located in various computer laboratories in The Ohio State University, Department of Computer and Information Science.

5.2. Bounding the maximum time difference

As noted previously, γ^k can increase as the network evolves. Numerical simulations indicate that in most cases γ^k decreases as k increases, but for some initial conditions γ^k increases with k . We want to know if there is some range of initial conditions along LLB such that γ^k does not increase with time. This would be useful in determining the amount of time a block oscillators spends in the active phase, and thus would play an important role in determining network parameters. If there were such a constraint, then one

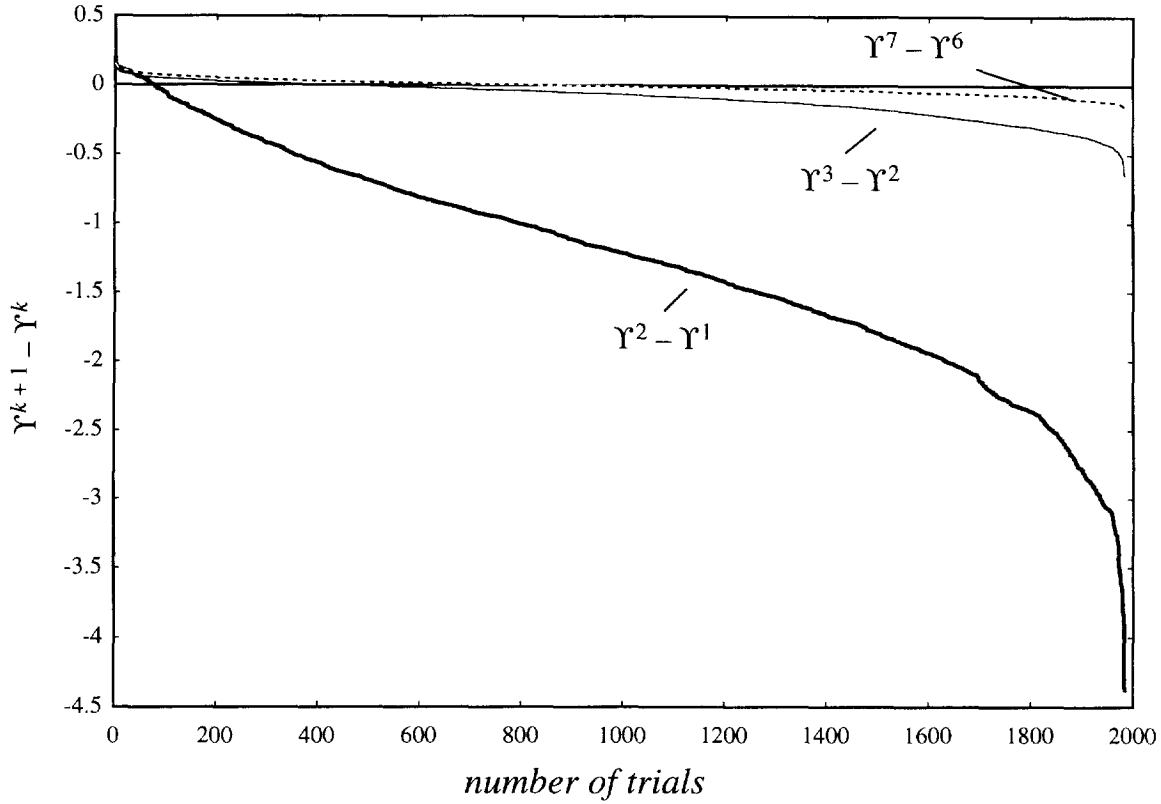


Fig. 14. A plot of the evolution of the maximum time difference for 1980 trials. The trials are arranged in order from largest to smallest to emphasize that most of the trials resulted in a decrease in γ^k . The thick line is a plot of $\gamma^2 - \gamma^1$ and $\gamma^3 - \gamma^2$ is indicated by the thin line. The network is almost stable by the third cycle and the change in $\gamma^3 - \gamma^2$ is not nearly as great as for $\gamma^2 - \gamma^1$. The dotted line displays $\gamma^7 - \gamma^6$. The parameters used are the same as in the caption of Fig. 7 with the exceptions that $\lambda = 7$ and $\tau = 0.04T$.

could always begin the oscillators within this range and know for certain that γ^k will not increase as the system evolves, in spite of coupling delays between neighboring oscillators.

Specifically, we explore whether there exists some range of initial conditions, which we call Ω , such that if N oscillators are randomly distributed within Ω , then,

$$\gamma^1 \geq \gamma^k. \quad (17)$$

Let Ω be a range of initial conditions on the LLB defined as $\Omega = [\Omega_B, \Omega_T]$, so that $\Omega_T - \Omega_B$ is the time it takes to traverse Ω . If $\Omega_T - \Omega_B \leq \tau$, then the time difference between every pair of oscillators in the network satisfies $\Gamma(y_i(0), y_j(0)) \leq \tau$ and the interaction term does not cause any oscillators to jump

up or down. Since the interaction does not change the time difference between any oscillators, the maximum time difference does not change, or $\gamma^1 = \gamma^k$. We conjecture a large range

$$\Omega_C = [0, t_{ps}], \quad (18)$$

where

$$t_{ps} = \log \left(\frac{c_1 + 2\gamma e^\tau}{c_2} \right). \quad (19)$$

The value of t_{ps} originates from analysis of two oscillators. It is the time difference resulting in perfect synchronization for a pair of oscillators. Simulations of oscillator networks, with random initial conditions in the range Ω_C , support this conjecture. In Fig. 14 we plot values of $\gamma^2 - \gamma^1$ (thick solid line) for 1980

trials of a chain of 75 oscillators randomly positioned so that the initial time difference between every pair of oscillators is within Ω_C . The values of $\Upsilon^2 - \Upsilon^1$ have been plotted in order from largest to smallest for simplicity. By far, the majority of trials yield a negative result for $\Upsilon^2 - \Upsilon^1$, indicating that the value of Υ^k decreases from the first to second period. Approximately 4% of the trials did, however, yield positive values for $\Upsilon^2 - \Upsilon^1$. The largest positive change and a value of 0.1905. The numerical method used was an adaptive Runge–Kutta method modified from [27] for time delay differential equations. The resulting average step size of the method was 0.1305. Errors in computing the Υ^k are on the order of the average step size. The small percentage of trials that resulted in small positive values of $\Upsilon^2 - \Upsilon^1$ are very likely to have resulted from numerical inaccuracy. In Fig. 14, $\Upsilon^3 - \Upsilon^2$ is given by the thin solid line. Note that there is less of a change from the second to third cycle because the network achieves stability quickly. The average number of cycles needed to achieve stability is 4, so the values of $\Upsilon^7 - \Upsilon^6$ should be near zero. In Fig. 14 the dotted line represents $\Upsilon^7 - \Upsilon^6$, and although near zero, it has noticeable deviations. The deviations from zero are again on the order of the average step size. This provides further evidence that numerical errors cause the deviations seen in both $\Upsilon^7 - \Upsilon^6$ and $\Upsilon^2 - \Upsilon^1$. We have tested this result with networks of 25, 50, and 100 oscillators as well, and display only one graph because the others are extremely similar and little additional information is revealed. We have also tested this algorithm with a fourth order Runge–Kutta algorithm with fixed step size. Similar results were obtained. Approximately 5% of the trials resulted in small positive increases in $\Upsilon^2 - \Upsilon^1$. Using this numerical algorithm, the maximum increase was $15h$ with step-size $h = 0.005$. We attribute these small increases to the fact that our conjecture is based on the singular limit $\varepsilon \rightarrow 0$, while in simulations, the value used was $\varepsilon = 0.025$.

In summary, our extensive simulations support our conjecture that Ω_C is a range of initial conditions which satisfies condition (17). Further examination of this conjecture also lends support. For ranges larger than Ω_C , a significant percentage of trials result in

$\Upsilon^2 - \Upsilon^1 > 1$. For ranges smaller than Ω_C there are specific initial conditions in which (17) is violated. But these conditions do not cause an increase when the range becomes as large as Ω_C . We note that parameters can be chosen so that the range Ω_C is a significant percentage of the period.

6. Concluding remarks

We have presented analysis describing the dynamics of a pair of relaxation oscillators with time delay coupling. We have proven that loosely synchronous solutions exist dependent on the initial conditions, the time delay, and the strength of the coupling. We have provided explicit statements regarding appropriate initial conditions, time delays, and coupling strengths which result in loose synchrony. Analysis and numerical simulations indicate that there is a critical time delay $\tau_{RM}/2$, beyond which antiphase solutions of period less than T commonly arise. Although the analysis for multiple oscillators has not been carried out, numerical simulations indicate that locally coupled networks of oscillators also display similar behaviors as seen in a pair of oscillators. In particular, loose synchrony exists between neighboring oscillators.

The behaviors analyzed and simulated in this paper are in terms of a specific set of relaxation oscillators. However, the behaviors we examined should also exist in other relaxation oscillators. In preliminary investigations of locally coupled networks of Morris–Lecar oscillators [23], Bonhoeffer–van der Pol oscillators [7], and other relaxation type oscillators, we find that loose synchrony is quickly attained for time delays less than the time spent on the fastest branch of the system. Both the Morris–Lecar and Bonhoeffer–van der Pol are related to the class of excitable-oscillatory systems including the Hodgkin–Huxley model of neuronal activity [10], and some of the behaviors seen here may carry over to this more complex model.

To characterize the degree of synchrony in the network as a whole, we have introduced a measure of synchrony, the maximum time difference between any two oscillators in the network. The maximum time difference of a network depends on the initial conditions

of the oscillators. In order to study the maximum time difference, we have given histograms of this measure using random initial conditions for several networks. Our results indicate that the maximum time difference typically decreases as the system evolves, and rarely reaches its maximum possible value, $(N - 1)\tau$. This observation holds even for small networks, where the initial time difference between oscillators can be greater than $(N - 1)\tau$. But our results indicate that some initial conditions exist which cause relatively large increases in the maximum time difference. In an effort to bound the maximum time difference we have postulated a range of initial conditions in which the maximum time difference does not increase. This range arises naturally from the analysis of a pair of oscillators and our extensive numerical experiments support this conjecture.

Below a certain connection strength, a pair of oscillators can exhibit neutrally stable desynchronous solutions. This result is in agreement with the results of [15]. With this result we found an analogous behavior to that of fractured synchrony described in [34]. Above the critical time delay, a pair of oscillators typically displays antiphase behavior with a frequency that can be significantly higher than the frequency of the synchronous solution. In networks of oscillators, with $\tau > \tau_{RM}/2$, antiphase, loosely synchronous, and other more complex behaviors are seen in numerical simulations.

We have tested a network equivalent to LEGION with time delays in the coupling between neighboring oscillators, and found that groups of oscillators can be desynchronized. However, the number of groups that can be segmented by LEGION decreases when time delays are introduced. This is because oscillator groups are no longer perfectly synchronous. The ability of LEGION to segment oscillator groups is related to the maximum time difference within each group. With our knowledge of a range of initial conditions in which the maximum time difference does not increase, we can choose appropriate parameters and initial conditions so that the properties of oscillatory correlation in LEGION are maintained.

Because relaxation oscillators capture some basic neuronal properties and time delays are inevitable in

neuronal signal transmission, our results should have implications to understanding oscillations in the nervous system. Our study suggests that in the presence of time delays local connections alone may be incapable of supporting precise synchronization over large neuronal populations. This may explain why synchrony is not seen across distances of more than 7 mm in the cat visual cortex, where lateral connections within the cortex are assumed to give rise to the observed synchronization [32]. Also, measurements of synchrony in neural activities indicate that synchrony is not perfect [32]. This imperfect synchronization might indicate the existence of loose synchrony because lateral connections always have time delays.

Acknowledgements

The authors would like to thank C. Jayaprakash for many useful conversations. This work is supported by an ONR grant (N00014-93-1-0335) and an NSF grant (IRI-9423312), and an ONR Young Investigator Award (N00014-96-1-0676) to DLW.

Appendix A

For regions II and III in Fig. 4, we show, in the singular limit, that as system (3) evolves, the time difference between the oscillators decreases. In region IV, we find that the time difference between the oscillators decreases only if the coupling strength is above a certain value, which we derive. Calculating how the time difference between the oscillators changes involves both ‘jump-up’ and ‘jump-down’ cases. The jump-up case is analyzed here, while the jump-down case is analyzed in Appendix B. Analysis in both appendices is for time delays $0 \leq \tau < \tau_{RM}/2$.

A.1. Region II

In region II, O_1 jumps up, and the initial position of O_2 is such that when it receives excitation at time τ later, it jumps up directly to URB. This activity is displayed in Fig. 5(B). This region is bounded by $\tau <$

$t_0 \leq \tau_1 + \tau$, where we use t_0 to denote the initial time difference between the two oscillators. Assuming that O_1 jumps up at time $t = 0$, and using (8) and (9), the positions of O_1 and O_2 at time τ are given by

$$\begin{aligned} y_1(\tau) &= (LLK_y - \lambda - \gamma)e^{-\tau} + \lambda + \gamma \\ &= c_1 e^{-\tau} + \lambda + \gamma, \end{aligned} \quad (\text{A.1})$$

$$y_2(\tau) = (y_2(0) - \lambda + \gamma)e^{-\tau} + \lambda - \gamma. \quad (\text{A.2})$$

We rewrite $y_2(0)$ in terms of t_0 , yielding

$$(LLK_y - \lambda + \gamma)e^{t_0} = c_2 e^{t_0} = (y_2(0) - \lambda + \gamma). \quad (\text{A.3})$$

Using (A.3), we rewrite (A.2) as

$$y_2(\tau) = c_2 e^{t_0 - \tau} + \lambda - \gamma. \quad (\text{A.4})$$

To find the time difference between the oscillators after they have jumped up to the active phase, t_1 , we use (9) to write

$$y_2(\tau) = (y_1(\tau) - \lambda - \gamma)e^{-t_1} + \lambda + \gamma. \quad (\text{A.5})$$

Substituting (A.1) and (A.4) into (A.5) yields

$$c_2 e^{t_0 - \tau} - 2\gamma = c_1 e^{-\tau - t_1}. \quad (\text{A.6})$$

We use (A.6) to write t_1 as a function of the initial time difference, t_0 ,

$$t_1 = \log \left[\frac{c_1 e^{-\tau}}{c_2 e^{t_0 - \tau} - 2\gamma} \right] = g(t_0). \quad (\text{A.7})$$

This equation arises when the order of the oscillators has been switched, i.e. O_2 leads O_1 . Only in this case can the time difference between the oscillators become larger than τ . It can be shown that initial conditions in region II always map into the analogous region on the URB, called region II_R. The equation for determining the time difference between the oscillators after the jump-down to the silent phase is given in (B.4). Using both (A.7) and (B.4) we can explicitly write the time difference between the oscillators after they return to the silent phase, t_2 , as a function of the initial time difference, t_0 ,

$$\begin{aligned} t_2 &= f(g(t_0)) \\ &= \log \left[\frac{c_8 e^{-\tau} (c_2 e^{t_0 - \tau} - 2\gamma)}{c_1 c_7 e^{-2\tau} + 2\gamma (c_2 e^{t_0 - \tau} - 2\gamma)} \right]. \end{aligned} \quad (\text{A.8})$$

After some tedious algebra it can be shown that $t_0 > t_2$ for all values of $t_0 > 0$ in region II.

A.2. Region III

We now examine region III, which is defined by

$$\tau_1 + \tau < t_0 < \tau_1 + \tau_{\text{RM}} - \tau, \quad (\text{A.9})$$

where τ_{RM} is given in (12) and τ_1 is given in (13). In this region, O_1 jumps up at time $t = 0$ and O_2 receives excitation at a time τ later. O_2 is far up enough on LLB such that it hops to ULB before jumping up to URB. Typical trajectories for a pair of oscillators in this region are displayed in Fig. 5(C). In this case we calculate the positions of the oscillators as follows:

$$\begin{aligned} y_1(t_0 - \tau_1) &= (LLK_y - \lambda - \gamma)e^{\tau_1 - t_0} + \lambda + \gamma \\ &= c_1 e^{\tau_1 - t_0} + \lambda + \gamma, \end{aligned} \quad (\text{A.10})$$

$$y_2(t_0 - \tau_1) = LLK_y + \alpha. \quad (\text{A.11})$$

To find the time difference between the oscillators on the active phase, t_1 , we use (9) to write

$$c_1 e^{\tau_1 - t_0} = (LLK_y + \alpha - \lambda - \gamma)e^{-t_1} = c_5 e^{-t_1}. \quad (\text{A.12})$$

We use (A.12) to write t_1 as a function of the initial time difference, t_0 ,

$$t_1 = t_0 - \tau_1 - \tau_5, \quad (\text{A.13})$$

where

$$\tau_5 = \log \left(\frac{c_1}{c_5} \right). \quad (\text{A.14})$$

In this case it can be shown that the values of t_1 can be in both region II_R and III_R. We do not examine region II_R as these time differences can be shown to always map to region II, and then the time difference between the oscillators always decreases as discussed previously. We now examine the time difference between the oscillators when they map from region II to region III_R. Using (A.13) and (B.9) we write the time difference between the oscillators after they have both returned to the silent phase, t_2 , as

$$t_2 = t_0 - \tau_1 - \tau_5 - \tau_2 - \tau_4. \quad (\text{A.15})$$

The values of τ_2 and τ_4 arise from the analysis of the jump-down and are given in (B.1) and (B.10), respectively. We examine what values of t_0 result in a value of t_1 that is in region III_R, or

$$t_1 > \tau_2 + \tau, \quad (\text{A.16})$$

$$t_0 - \tau_1 - \tau_5 > \tau_2 + \tau, \quad (\text{A.17})$$

$$t_0 > \tau_1 + \tau_5 + \tau_2 + \tau. \quad (\text{A.18})$$

If t_2 is positive, then (A.15) shows that the time difference between the oscillators after a single period has decreased. However, if t_2 is negative, we must test if it is possible for $|t_2| > t_0$. We examine the following inequality:

$$t_2 = t_0 - \tau_1 - \tau_5 - \tau_2 - \tau_4 > -t_0, \quad (\text{A.19})$$

$$2t_0 > \tau_1 + \tau_5 + \tau_2 + \tau_4. \quad (\text{A.20})$$

Using (A.20) and the minimum value of t_0 , from (A.18), results in

$$2(\tau_1 + \tau_5 + \tau_2 + \tau) > \tau_1 + \tau_5 + \tau_2 + \tau_4, \quad (\text{A.21})$$

$$\tau_1 + \tau_5 + \tau_2 + 2\tau > \tau_4, \quad (\text{A.22})$$

Since $\tau_1 > \tau_4$, (A.22) is always true, and therefore $|t_2| < t_0$. Thus, the oscillators in region III always experience a decrease in the absolute value of their time difference after jumping up and down.

A.3. Region IV

The last case we examine on LLB is for initial conditions such that O_1 jumps up to URB and down to LLB, while O_2 remains on the silent phase (see Fig. 5(D)). This region is defined by the following bounds:

$$\tau_1 + \tau_{\text{RM}} + \tau < t_0 \leq \tau_{\text{LLB}} - \tau, \quad (\text{A.23})$$

where τ_{LLB} is given in (11). The leading oscillator, O_1 , jumps up at time $t = 0$, and the positions of the oscillators after O_1 traverses LRB are

$$y_1(\tau_{\text{RM}}) = LRK_y, \quad (\text{A.24})$$

$$y_2(\tau_{\text{RM}}) = c_2 e^{t_0 - \tau_{\text{RM}}} + \lambda - \gamma. \quad (\text{A.25})$$

To find the time difference between the oscillators when they are both on the silent phase, t_2 , we use (8) to write

$$LRK_y = c_2 e^{t_0 - \tau_{\text{RM}} - t_2} + \lambda - \gamma. \quad (\text{A.26})$$

We use (A.26) to write t_2 as a function of t_0 ,

$$t_2 = t_0 - \tau_6 - \tau_{\text{RM}} \quad (\text{A.27})$$

with

$$\tau_6 = \log \left(\frac{c_4}{c_2} \right). \quad (\text{A.28})$$

If t_2 is positive, then a decrease in the time difference between the oscillators occurs. However, if t_2 is negative, then O_2 leads O_1 , and we must check if $|t_2| > t_0$. We examine the following equation:

$$\tau_6 + \tau_{\text{RM}} - t_0 < t_0, \quad (\text{A.29})$$

$$t_0 > \frac{\tau_6 + \tau_{\text{RM}}}{2}. \quad (\text{A.30})$$

Using the minimum value of t_0 in region IV, the constraint (A.30) becomes

$$2(\tau_1 + \tau_{\text{RM}} + \tau) > \tau_6 + \tau_{\text{RM}} \quad (\text{A.31})$$

or

$$\tau_6 < 2\tau_1 + \tau_{\text{RM}} + 2\tau, \quad (\text{A.32})$$

$$\frac{c_4}{c_2} < \left(\frac{c_6}{c_2} \right)^2 \frac{c_1}{c_3} e^{2\tau}, \quad (\text{A.33})$$

$$c_6^2 = (c_2 + \alpha)^2 > \frac{c_2 c_3 c_4}{c_1} e^{-2\tau}. \quad (\text{A.34})$$

We rewrite (A.34) as a restriction on the coupling strength

$$\alpha > \sqrt{\frac{c_2 c_3 c_4}{c_1}} e^{-\tau} - c_2. \quad (\text{A.35})$$

The above condition puts a limiting value on the minimum value of α . Below this value for the connection weight it is possible for $|t_2| > t_0$ and neutrally stable desynchronous solutions can result.

There is a part of region V that juts between region IV and region III. In region V, it is possible for antiphase solutions to arise dependent on the initial conditions, the time delay, and the coupling strength. We

examine whether a pair of oscillators with initial conditions in region IV will automatically map to region III, without entering region V. To test this we make the following statement:

$$t_2 = \tau_6 + \tau_{RM} - t_0 < \tau_1 + \tau_{RM} - \tau, \quad (\text{A.36})$$

$$\tau_6 - \tau_1 + \tau < t_0. \quad (\text{A.37})$$

Using (A.37) with the smallest value that t_0 can take in region IV, we write

$$\tau_6 - \tau_1 + \tau < \tau_1 + \tau_{RM} + \tau, \quad (\text{A.38})$$

$$\tau_6 - \tau_{RM} < 2\tau_1, \quad (\text{A.39})$$

$$\alpha > \sqrt{\frac{c_4 c_3}{c_1}} - c_2. \quad (\text{A.40})$$

If condition (A.40) is satisfied then the oscillators whose initial conditions are in region IV will not map into region V. We note that if condition (A.35) is satisfied, then automatically, (A.40) is satisfied. Thus for coupling strengths that result in loose synchrony, a pair of oscillators in region IV will never map to region V. Also, we note that it is not possible for O_1 to make two traversals of LRB because the maximum possible y -value for O_2 is $LRK_y + \alpha$.

If constraints (A.35) and the constraint derived in Appendix B, (B.14), are satisfied then the oscillators whose initial time difference is in regions II–IV of Fig. 4, will eventually have a time difference of less than or equal to the time delay, i.e. they will be loosely synchronous.

Appendix B

We calculate how the time difference between the oscillators changes as they jump-down from the active phase to the silent phase. We label the two regions II_R and III_R because of their correspondence to regions II and III of Fig. 4. No other trajectories are possible since we have assumed that the fastest branch of the system is LRB.

B.1. Region II_R

We assume that O_1 jumps down first, at time $t = 0$, then O_2 ceases to receive excitation at time τ and

jumps down to LLB (Fig. 5(E)). The time difference between the oscillators in region II_R is bounded by $\tau < t_1 \leq \tau_2 + \tau$, where

$$\tau_2 = \log\left(\frac{c_3}{c_7}\right). \quad (\text{B.1})$$

The positions of the oscillators immediately after the jump-down are given by

$$y_1(\tau) = c_8 e^{-\tau} + \lambda - \gamma, \quad (\text{B.2})$$

$$y_2(\tau) = c_7 e^{t_1 - \tau} + \lambda + \gamma. \quad (\text{B.3})$$

The time difference between the oscillators after they are both on the silent phase, t_2 , is given by

$$t_2 = \log\left[\frac{c_8 e^{-\tau}}{c_7 e^{t_1 - \tau} + 2\gamma}\right] = f(t_1). \quad (\text{B.4})$$

It can be shown that the oscillators whose initial conditions are in region II_R always map to region II of Fig. 4.

B.2. Region III_R

The second case to examine is the region

$$\tau_2 + \tau < t_1 \leq \tau_2 + \tau_{RM} - \tau, \quad (\text{B.5})$$

where τ_{RM} is defined in (12). In this region, O_1 jumps down, and the initial separation between the oscillators is such that O_2 hops to LRB before jumping down to LLB. Trajectories for a pair of oscillators in this region are shown in Fig. 5(F). The positions of the oscillators when they are both on LLB are given by

$$\begin{aligned} y_1(t_1 - \tau_2) &= (LRK_y + \alpha - \lambda + \gamma)e^{\tau_2 - t_1} + \lambda - \gamma \\ &= c_8 e^{\tau_2 - t_1} + \lambda - \gamma, \end{aligned} \quad (\text{B.6})$$

$$y_2(t_1 - \tau_2) = LRK_y. \quad (\text{B.7})$$

To find the time difference between the oscillators when they are both on the silent phase, t_2 , we use (8) to write

$$c_8 e^{\tau_2 - t_1} = c_4 e^{-t_2} \quad (\text{B.8})$$

resulting in

$$t_2 = t_1 - \tau_2 - \tau_4, \quad (\text{B.9})$$

where

$$\tau_4 = \log\left(\frac{c_8}{c_4}\right). \quad (\text{B.10})$$

Other trajectories can arise during the jump-down, but not with the assumptions that LRB is the fastest branch in the system. This assumption implies that the following condition must be true:

$$\tau_{\text{RM}} < \tau_9, \quad (\text{B.11})$$

where

$$\tau_9 = \log\left(\frac{c_8}{c_6}\right). \quad (\text{B.12})$$

From condition (B.11) we derive the following bound on the coupling strength:

$$\frac{c_1}{c_2} < \frac{c_4 + \alpha}{c_2 + \alpha}, \quad (\text{B.13})$$

$$\alpha < \frac{c_1 c_2 - c_3 c_4}{c_3 - c_1}. \quad (\text{B.14})$$

References

- [1] K. Bar-Eli, On the stability of coupled chemical oscillators, *Physica D* 14 (1985) 242–252.
- [2] S. Campbell and D.L. Wang, Synchronization and desynchronization in a network of locally coupled Wilson–Cowan oscillators, *IEEE Trans. Neural Net.* 7 (1996) 541–554.
- [3] T. Chawanya, T. Aoyagi, I. Nishikawa, K. Okuda and Y. Kuramoto, A model for feature linking via collective oscillations in the primary visual cortex, *Biol. Cybern.* 68 (1993) 483–490.
- [4] A.H. Cohen, P.J. Holmes and R.H. Rand, The nature of the coupling between segmental oscillators of the lamprey spinal generator for locomotion: A mathematical model, *J. Math. Biol.* 13 (1982) 345–349.
- [5] A. Destexhe and P. Gaspard, Bursting oscillations from a homoclinic tangency in a time delay system, *Phys. Lett. A* 173 (1993) 386–391.
- [6] U. Ernst, K. Pawelzik and T. Geisel, Synchronization induced by temporal delays in pulse-coupled oscillators, *Phys. Rev. Lett.* 74 (1995) 1570–1573.
- [7] R. Fitzhugh, Impulses and physiological states in theoretical models of nerve membrane, *Biophys. J.* 1 (1961) 445–466.
- [8] J. Foss, A. Longtin, B. Mensour and J. Milton, Multistability and delayed recurrent loops, *Phys. Rev. Lett.* 76 (1996) 708–711.
- [9] J. Grasman and M.J.W. Jansen, Mutually synchronized relaxation oscillators as prototypes of oscillating systems in biology, *J. Math. Biol.* 7 (1979) 171–197.
- [10] A.L. Hodgkin and A.F. Huxley, A quantitative description of membrane current and its application to conduction and excitation in nerve, *J. Physiol.* 117 (1952) 500–544.
- [11] D. Horn, D. Sagi and M. Usher, Segmentation, binding, and illusory conjunctions, *Neural Comp.* 3 (1991) 510–525.
- [12] S.R. Inamdar, V. Ravi Kumar and B.D. Kulkarni, Dynamics of reacting systems in presence of time delay, *Chem. Eng. Sci.* 46 (1991) 901–908.
- [13] E.R. Kandel, J.H. Schwartz and T.M. Jessell, *Principles of Neural Science*, 3rd Ed. (Elsevier, New York, 1991).
- [14] P. König and T.B. Schillen, Stimulus-dependent assembly formation of oscillatory responses: I. Synchrony, *Neural Comp.* 3 (1991) 155–166.
- [15] N. Kopell and D. Somers, Anti-phase solutions in relaxation oscillators coupled through excitatory interactions, *J. Math. Biol.* 33 (1995) 261–280.
- [16] Y. Kuang, *Delay Differential Equations with Applications in Population Dynamics* (Academic Press, Boston, 1993).
- [17] Y. Kuramoto, Cooperative dynamics of oscillator community, *Prog. Theoret. Phys.* 79 (1984) 223–240.
- [18] T. LoFaro, A period adding bifurcation in a pair of coupled neurons, Ph.D. Dissertation, Boston University (1994).
- [19] T.B. Luzyanina, Synchronization in an oscillator neural network model with time-delayed coupling, *Network* 6 (1995) 43–59.
- [20] N. MacDonald, *Biological Delay Systems: Linear Stability Theory* (Cambridge University Press, Cambridge, 1989).
- [21] P.M. Milner, A model for visual shape recognition, *Psychol. Rev.* 81 (1974) 521–535.
- [22] R.E. Mirollo and S.H. Strogatz, Synchronization of pulse-coupled biological oscillators, *SIAM J. Appl. Math.* 50 (1990) 1645–1662.
- [23] C. Morris and H. Lecar, Voltage oscillations in the barnacle giant muscle fiber, *Biophys. J.* 35 (1981) 193–213.
- [24] E. Neibur, H.G. Schuster and D.M. Kammen, Collective frequencies and metastability in network of limit-cycle oscillators with time delay, *Phys. Rev. Lett.* 67 (1991) 2753–2756.
- [25] P.F. Pinsky and J. Rinzel, Synchrony measures for biological neural networks, *Biol. Cybern.* 73 (1995) 129–137.
- [26] R.E. Plant, A. Fitzhugh differential-difference equations modeling recurrent neural feedback, *SIAM J. Appl. Math.* 40 (1981) 150–162.
- [27] W.H. Press, S.A. Teukolsky, W.T. Vetterling and B.P. Flannery, *Numerical Recipes in C: The Art of Scientific Computing*, 2nd Ed. (Cambridge University Press, New York, 1992).
- [28] T.B. Schillen and P. König, Stimulus-dependent assembly formation of oscillator responses: II. Desynchronization, *Neural Comp.* 3 (1991) 167–178.
- [29] I. Schreiber and M. Marek, Strange attractors in coupled reaction–diffusion cells, *Physica D* 5 (1982) 258–272.
- [30] H.G. Schuster and P. Wagner, Mutual entrainment of two limit cycle oscillators with time delayed coupling, *Prog. Theoret. Phys.* 81 (1989) 939–945.

- [31] A. Shibata and N. Saito, Time delays and chaos in two competing species, *Math. Biosci.* 51 (1980) 199–211.
- [32] W. Singer and C.M. Gray, Visual feature integration and the temporal correlation hypothesis, *Ann. Rev. Neurosci.* 18 (1995) 555–586.
- [33] D. Somers and N. Kopell, Rapid synchronization through fast threshold modulation, *Biol. Cybern.* 68 (1993) 393–407.
- [34] D. Somers and N. Kopell, Waves and synchrony in networks of oscillators of relaxation and non-relaxation type, *Physica D* 89 (1995) 169–183.
- [35] H. Sompolinsky and M. Tsodyks, Segmentation by a network of oscillators with stored memories, *Neural Comp.* 6 (1994) 642–657.
- [36] D. Terman and D.L. Wang, Global competition and local cooperation in a network of neural oscillators, *Physica D* 81 (1995) 148–176.
- [37] C. von der Malsburg, The correlation theory of brain functions, Internal Report 81-2, Max-Planck-Institute for Biophysical Chemistry, Göttingen, FRG (1981).
- [38] C. von der Malsburg and W. Schneider, A neural cocktail-party processor, *Biol. Cybern.* 54 (1986) 29–40.
- [39] D.L. Wang, Modeling global synchrony in the visual cortex by locally coupled neural oscillators, *Proc. 15th Ann. Conf. Cognit. Sci. Soc. (Boulder Co., 1993)* 1058–1063.
- [40] D.L. Wang, Emergent synchrony in locally coupled neural oscillators, *IEEE Trans. Neural Networks* 6 (1995) 941–948.
- [41] D.L. Wang, J. Buhmann and C. von der Malsburg, Pattern segmentation in associative memory, *Neural Comp.* 2 (1990) 94–106.
- [42] D.L. Wang and D. Terman, Locally excitatory globally inhibitory oscillator networks, *IEEE Trans. Neural Networks* 6 (1995) 283–286.
- [43] K. Wiesenfeld, P. Colet and S.H. Strogatz, Synchronization transitions in a disordered Josephson series array, *Phys. Rev. Lett.* 76 (1996) 404–407.
- [44] H.R. Wilson and J.D. Cowan, Excitatory and inhibitory interactions in localized populations of model neurons, *Biophys. J.* 12 (1972) 1–24.
- [45] A.T. Winfree, Biological rhythms and the behavior of populations of coupled oscillators, *J. Theoret. Biol.* 16 (1967) 15–42.
- [46] S. Zeki, *A Vision of the Brain* (Blackwell, Oxford, 1993).